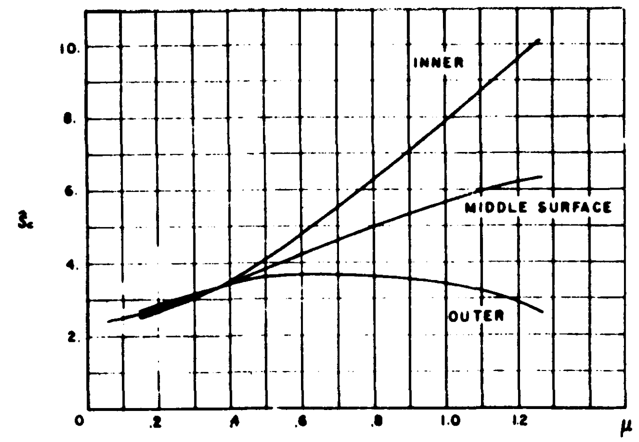

A—$\hat{S}_c$ for $\phi = 0$ vs. β_{ρ_0} (capped cylinder), $\nu = 0.3$

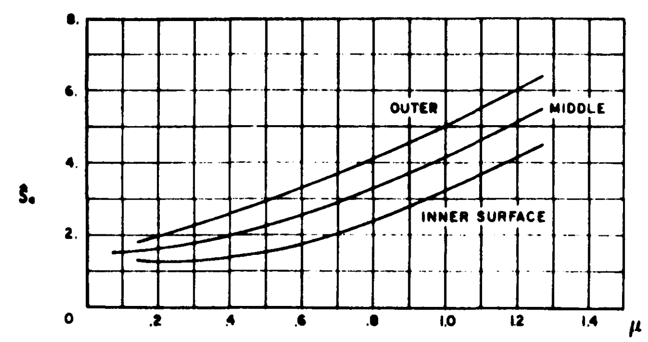

C—$\hat{S}_c$ for $\phi = \pi/4$ vs. β_{ρ_0} (capped cylinder), $\nu = 0.3$

NOTE
REFERENCE: "STATE OF STRESS IN A CIRCULAR CYLINDRICAL SHELL WITH A CIRCULAR HOLE," WELDING RESEARCH COUNCIL BULLETIN 102, 1965.

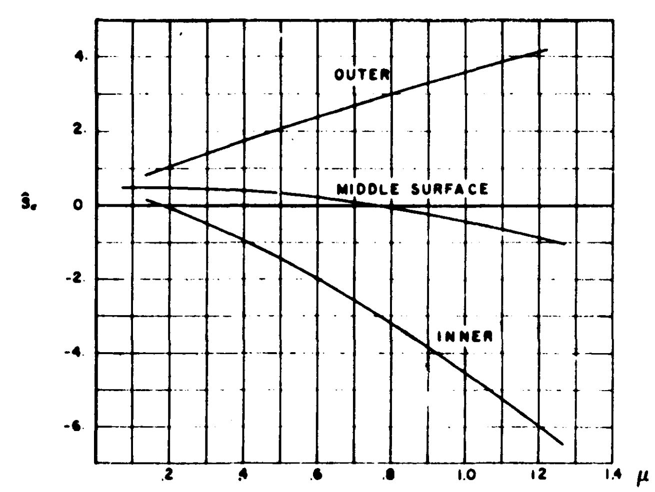

E—$\hat{S}_c$ for $\phi = \pi/2$ vs. β_{ρ_0} (capped cylinder), $\nu = 0.3$

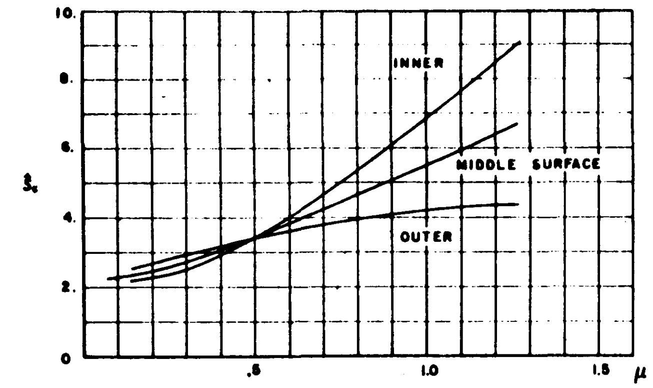

B—$\hat{S}_c$ for $\phi = \pi/8$ vs. β_{ρ_0} (capped cylinder), $\nu = 0.3$

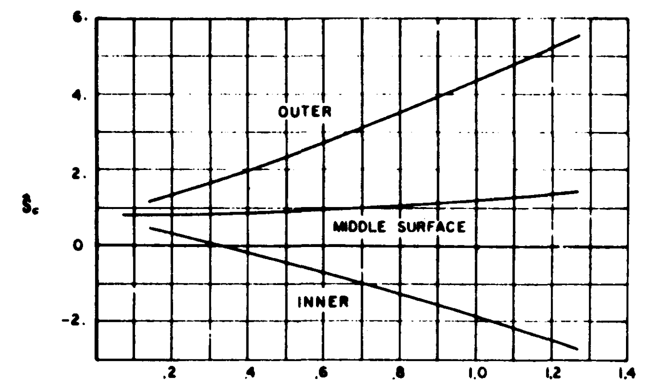

D—$\hat{S}_c$ for $\phi = 3\pi/8$ vs. β_{ρ_0} (capped cylinder), $\nu = 0.3$

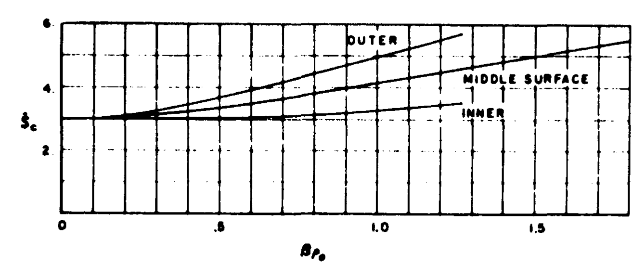

F—$\hat{S}_c$ at $\phi = \pi/2$ for Case II (extension case) vs. β_{ρ_0}, $\nu = 0.3$

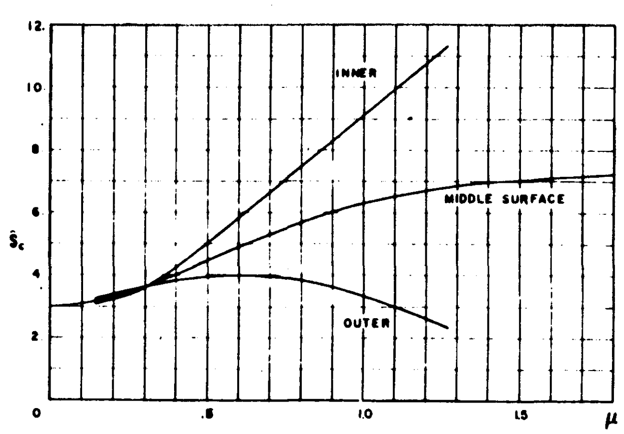

G—$\hat{S}_c$ at $\phi = 0$ for Case III (internal pressure), $\nu = 0.3$

GPU Nuclear **Update -1**

TMI Unit-1 **7/82**

Total Stress Concentration Factors for Given Loading Cases

Fig. 5C-1

Table 3—Stress Concentration Factor Variations for Different β_{μ} at Various Angles—Capped Cylinder

$\nu = 0.30$

β_{μ}	$(\hat{S}_c)$*upper*	S_c	$(\hat{S}_c)$*lower*
		$\phi = 0$	
0.14142	2.75054	2.64709	2.54365
0.21213	2.94174	2.81900	2.69625
0.28284	3.13290	3.03670	2.94050
0.35355	3.30842	3.28570	3.26297
0.42426	3.45933	3.55467	3.65001
0.49497	3.58032	3.83486	4.08940
0.56568	3.66795	4.11911	4.57027
0.63639	3.72044	4.40201	5.08357
0.70710	3.73656	4.67874	5.62091
0.84852	3.66013	5.20121	6.74228
0.98994	3.44158	5.66463	7.88769
1.13137	3.09080	6.05690	9.02300
1.27279	2.61996	6.37120	10.12243
		$\phi = \pi/8$	
0.14142	2.46986	2.33179	2.19372
0.21213	2.66925	2.47978	2.29030
0.28284	2.87265	2.67011	2.46758
0.35355	3.06813	2.89212	2.71611
0.42426	3.25013	3.13783	3.02553
0.49497	3.41623	3.40126	3.38629
0.56568	3.56589	3.67806	3.79024
0.63639	3.69959	3.96509	4.23059
0.70710	3.81810	4.25958	4.70107
0.84852	4.01561	4.86482	5.71403
0.98994	4.16952	5.48212	6.79472
1.13137	4.29120	6.10374	7.91627
1.27279	4.39120	6.72431	9.05741
		$\phi = \pi/4$	
0.14142	1.79394	1.56884	1.34374
0.21213	2.01190	1.65385	1.29580
0.28284	2.23906	1.76710	1.29514
0.35355	2.46909	1.90438	1.33966
0.42426	2.70142	2.06304	1.42466
0.49497	2.93776	2.24160	1.54544
0.56568	3.18071	2.43944	1.69816
0.63639	3.43312	2.65648	1.87983
0.70710	3.69754	2.89277	2.08800
0.84852	4.27107	3.42439	2.57771
0.98994	4.91382	4.03512	3.15642
1.13137	5.63074	4.72359	3.81643
1.27279	6.42060	5.48575	4.55090
		$\phi = 3\pi/8$	
0.14142	1.12040	0.80340	0.48640
0.21213	1.35527	0.81807	0.28087
0.28284	1.59750	0.83819	0.07888
0.35355	1.84227	0.86252	−0.11723
0.42426	2.08946	0.88996	−0.30954
0.49497	2.34032	0.91983	−0.50065
0.56568	2.59629	0.95182	−0.69263
0.63639	2.85862	0.98593	−0.88675
0.70710	3.12823	1.02243	−1.08337
0.84852	3.69078	1.10414	−1.48249
0.98994	4.28578	1.20142	−1.88293
1.13137	4.91210	1.31959	−2.27291
1.27279	5.56731	1.46418	−2.63894
		$\phi = \pi/2$	
0.21213	1.08342	0.46892	−0.14557
0.28284	1.32929	0.44570	−0.43787
0.35355	1.57420	0.41483	−0.74454
0.42426	1.81691	0.37473	−1.06744
0.49497	2.05720	0.32403	−1.40912
0.56568	2.29480	0.26158	−1.77164
0.63639	2.52926	0.18654	−2.15617
0.70710	2.75997	0.09861	−2.56273
0.84852	3.20626	−0.11635	−3.43897
0.98994	3.62829	−0.38079	−4.38968
1.13137	4.02201	−0.68968	−5.40137
1.27279	4.38777	−1.03524	−6.45627

Table 3-Continued

$\hat{S}_c$ (*Middle Surface only*)

β_{μ}	$\phi = 0$	$\pi/10$	$\pi/5$	$3\pi/10$	$2\pi/5$	$\pi/2$
1.4142	6.6163	7.1566	7.2307	4.7289	0.6424	−1.4030
1.5909	6.7936	7.7349	8.3542	5.6384	0.6623	−1.8994
1.7677	6.9050	8.4207	9.5285	6.6467	0.7164	−2.4293

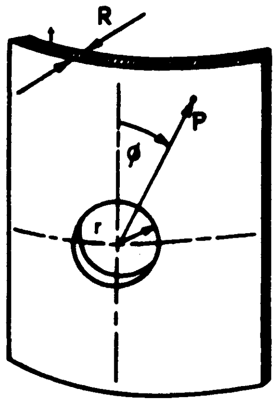

$$\mu = \frac{1}{2}\sqrt[4]{3(1-\nu^2)} \quad \frac{r}{\sqrt{Rt}}$$

The membrane stress concentration factor S_c and the total stress concentration factor $\hat{S}_c$ are, respectively, defined by

$$S_c = \frac{\text{largest of } (N_1, N_2)}{\text{largest of } (N_1^0, N_2^0)} = \hat{S}_c$$

(middle surface)

$$\hat{S}_c = \frac{\text{largest of } (\sigma 1, \sigma 2)}{\text{largest of } (\sigma 1^0, \sigma 2^0)} \quad \text{(for fixed } r, \phi)$$

where N_1^0, N_2^0 are the nominal principal stress resultants and $\sigma 1^0$, $\sigma 2^0$ are the nominal flexural stresses for the shell under the same loading but without the hole. N_1 and N_2 denote the principal stress resultants, σ_1 and σ_2 the principal stresses respectively. The stress concentration factor is calculated as a function of ϕ.

NOTE
REFERENCE: "STATE OF STRESS IN A CIRCULAR CYLINDRICAL SHELL WITH A CIRCULAR HOLE," WELDING RESEARCH COUNCIL BULLETIN 102, 1965.

GPU Nuclear — Update -1

TMI Unit-1 — 7/82

Stress Concentration Factor Variations for Different at Various Angles - Capped Cylinder

Fig. 5C-2

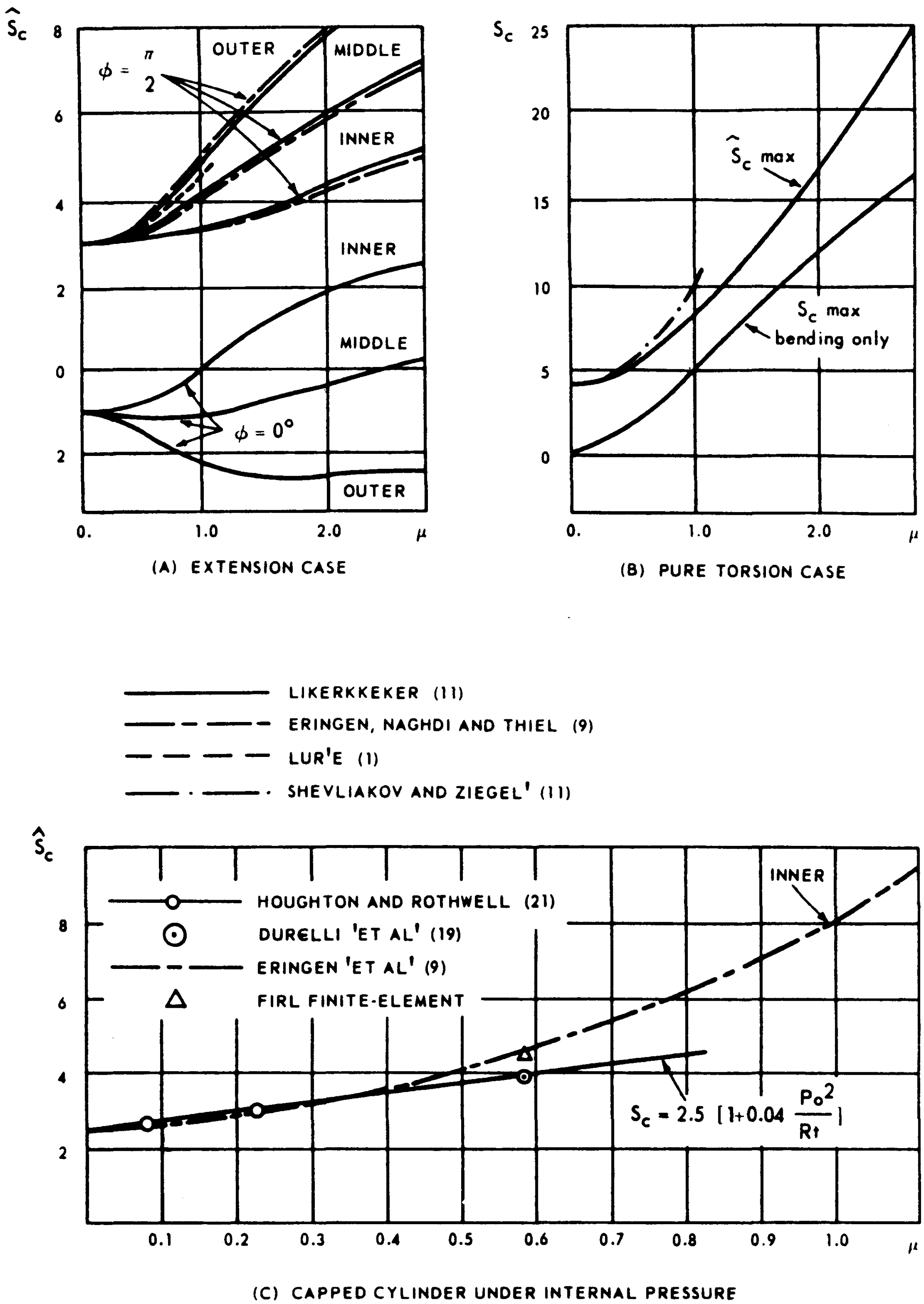

GPU Nuclear **Update -1**

TMI Unit-1 **7/82**

Stress Distribution around Openings in Cylindrical Shells

Fig. 5C-3

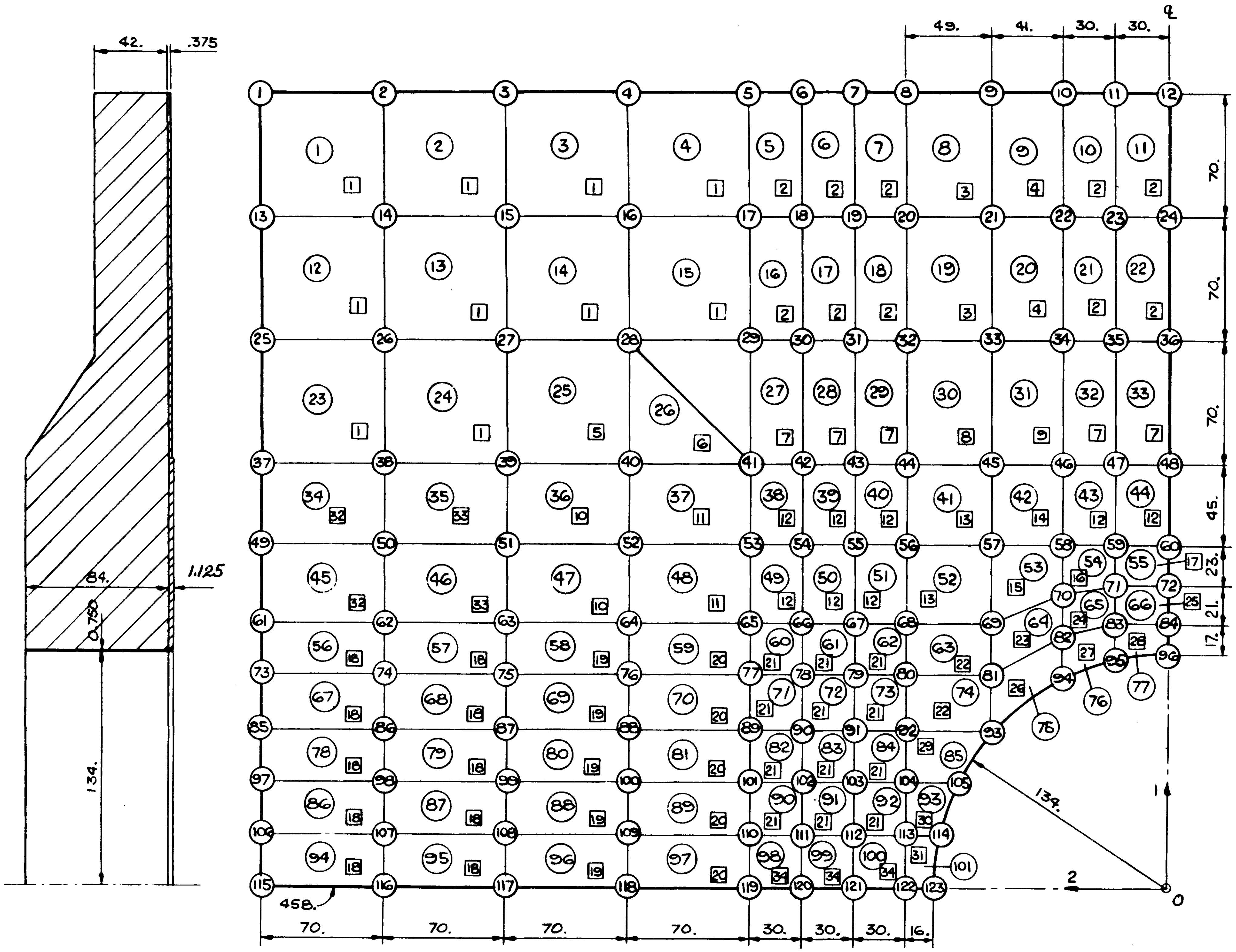

REFERENCES:

(5) NODAL POINT NUMBER

(15) PANEL NUMBER

[21] PANEL TYPE NUMBER

NOTE:
ALL DIMENSIONS ARE GIVEN IN INCHES

GPU Nuclear **Update - 1**

TMI Unit-1 **7/82**

Grid for Finite Element Analysis of Stresses Around Equipment Hatch in RCB

Fig. 5C-4

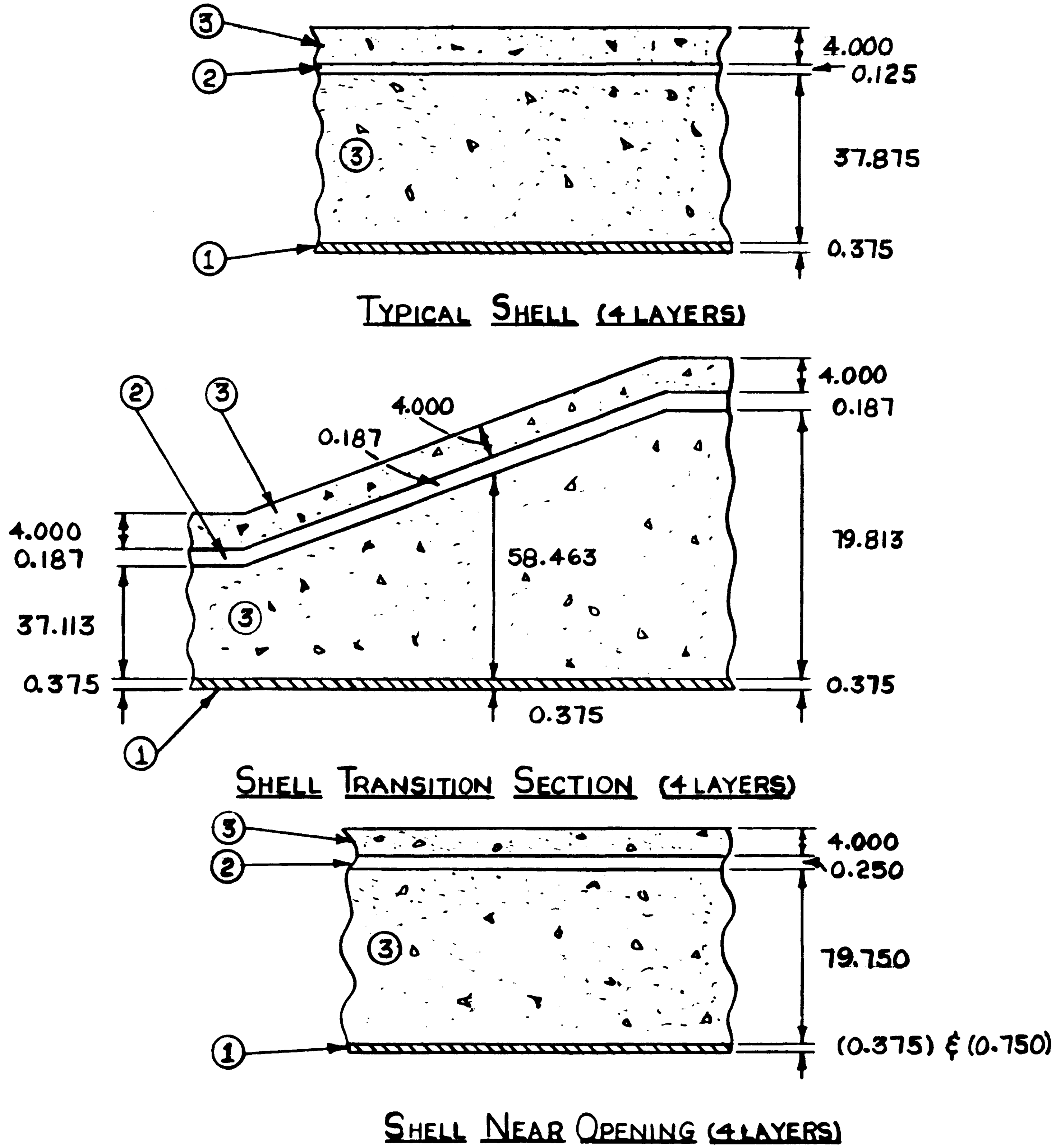

CODE DESIGNATION

① STEEL LINER

② REINFORCING STEEL

③ CONCRETE

① STEEL LINER

E_1 = 30,000 KSI

E_2 = 30,000 KSI

V_{12} = 0.3

G_{12} = 11,307 KSI

② REINFORCING STEEL

E_1 = 30,000 KSI

E_2 = 30,000 KSI

V_{12} = 0

G_{12} = 0

③ CONCRETE

E_1 = 4000 KSI

E_2 = 4000 KSI

V_{12} = 0.15 KSI

G_{12} = 1740 KSI

GPU Nuclear	Update -1
TMI Unit-1	7/82
Layer Thickness and Designation	
	Fig. 5C-5

EXPERIMENTAL ————
THEORETICAL
VAN DICKE, ERINGEN 'ET AL' —·—·—
FINITE ELEMENT SOLUTION – – – – –

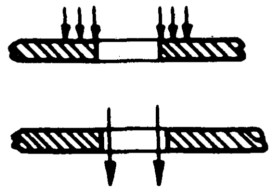

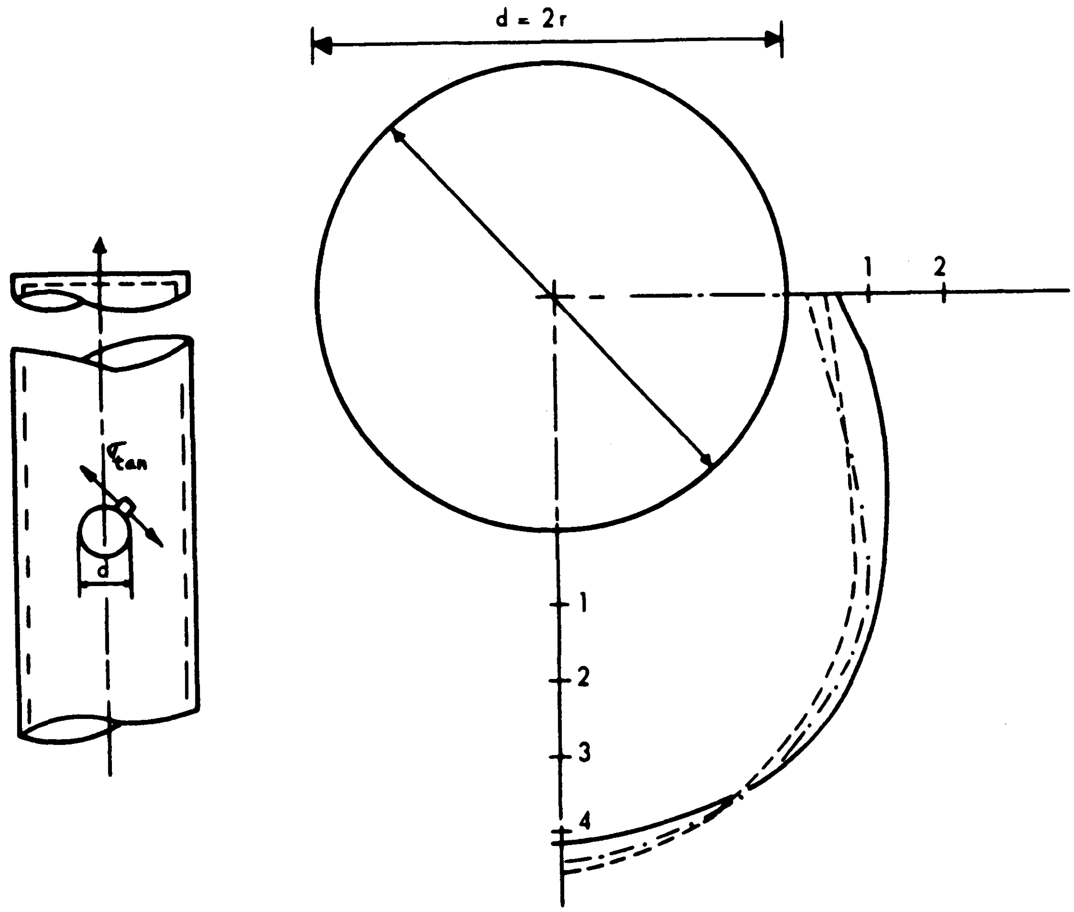

p. 5C.FIG-6

GPU Nuclear **Update -1**

TMI Unit-1 **7/82**

Member Stresses around Opening Edge (Vessel Subject to Internal Pressure)

Fig. 5C-6

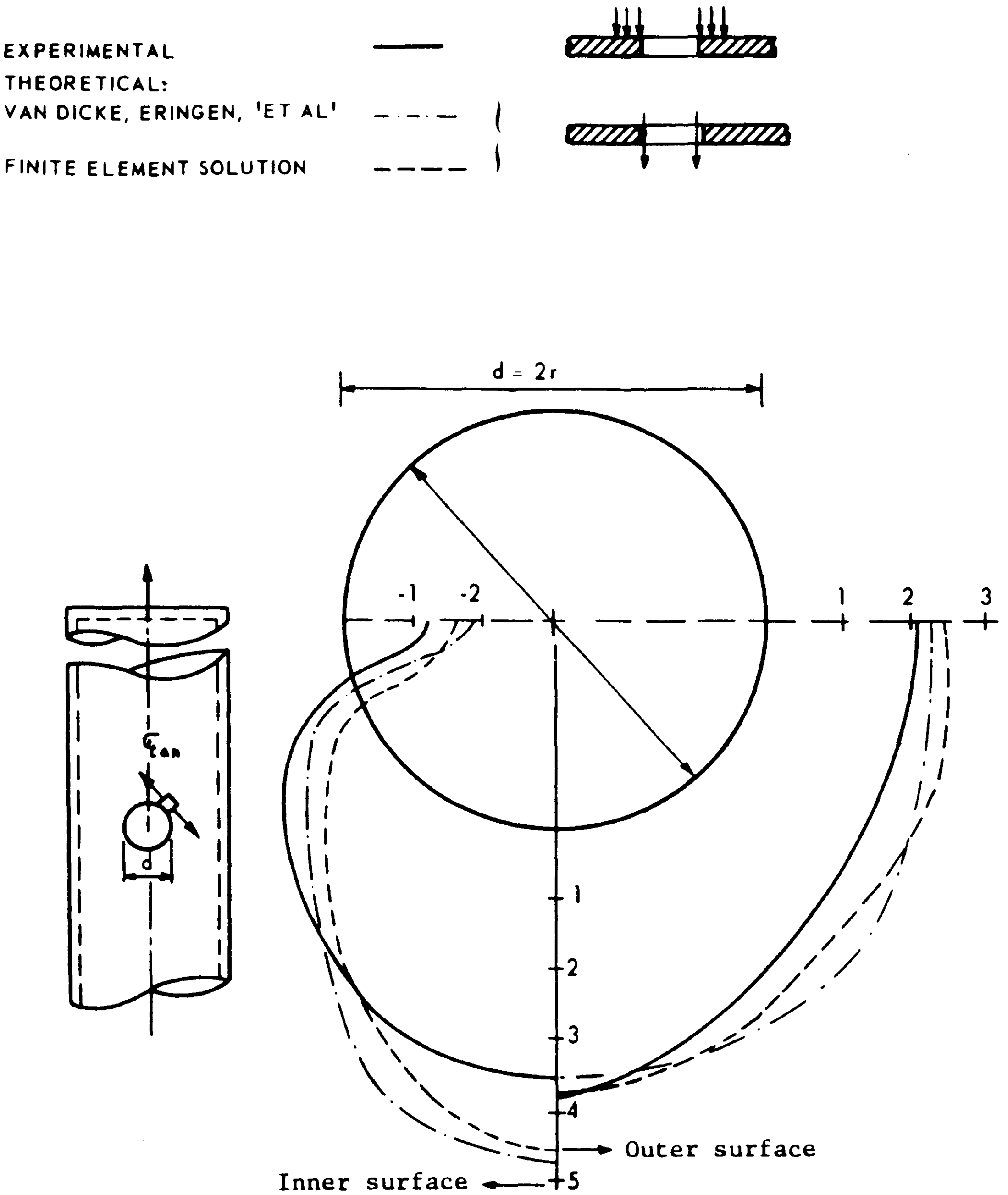

p. 5C.FIG-7

GPU Nuclear

TMI Unit-1

Update -1

7/82

Surface Stresses around Opening Edge (Vessel Subject to Internal Pressure)

Fig. 5C-7

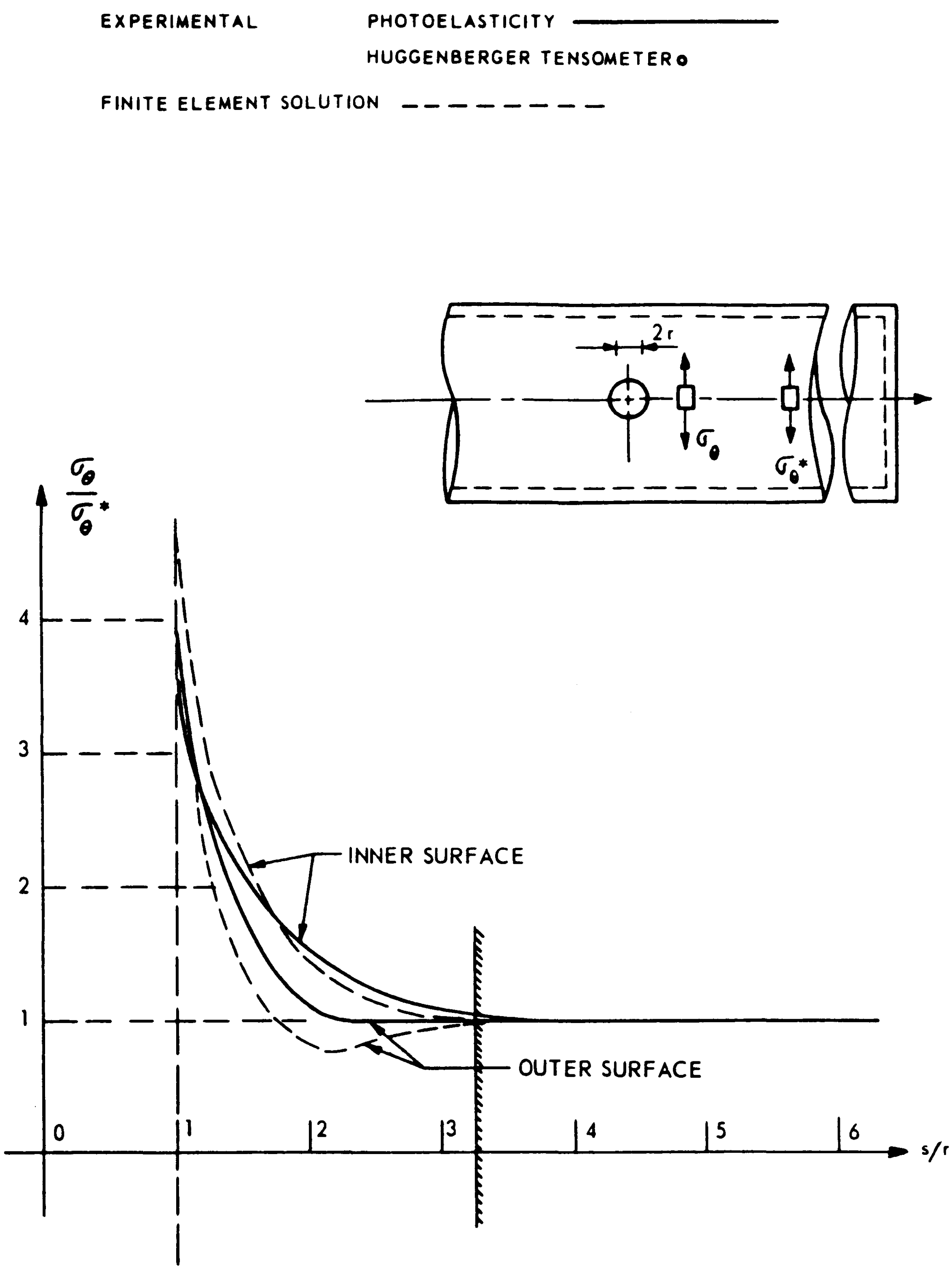

p. 5C.FIG-8

GPU Nuclear

TMI Unit-1

Update -1

7/82

Hoop Stresses along Longitudinal Axis (Vessel Subject to Internal Pressure)

Fig. 5C-8

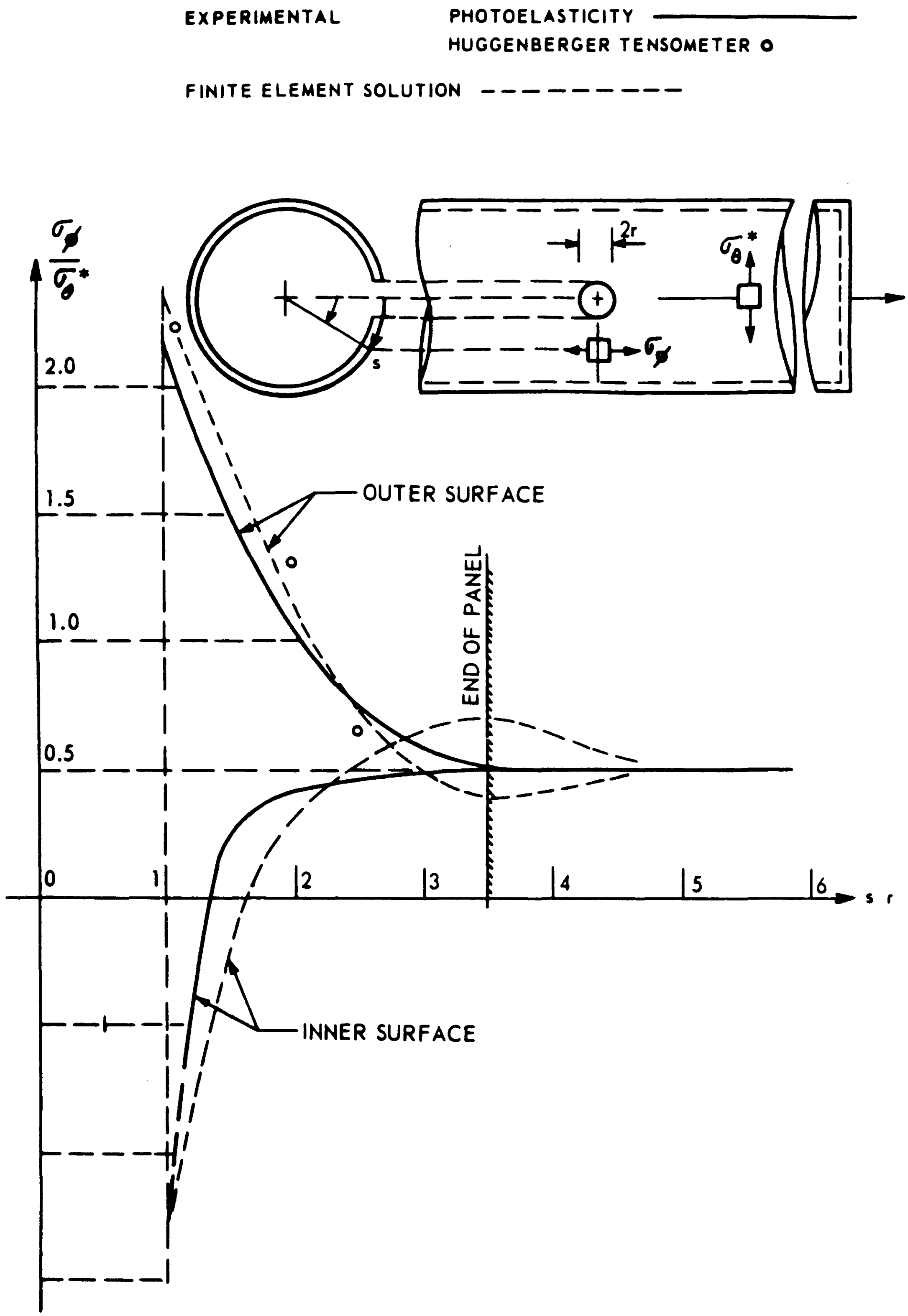

GPU Nuclear Update -1

TMI Unit-1 7/82

Axial Stresses along Transverse Axis (Vessel Subject to Internal Pressure)

Fig. 5C-9

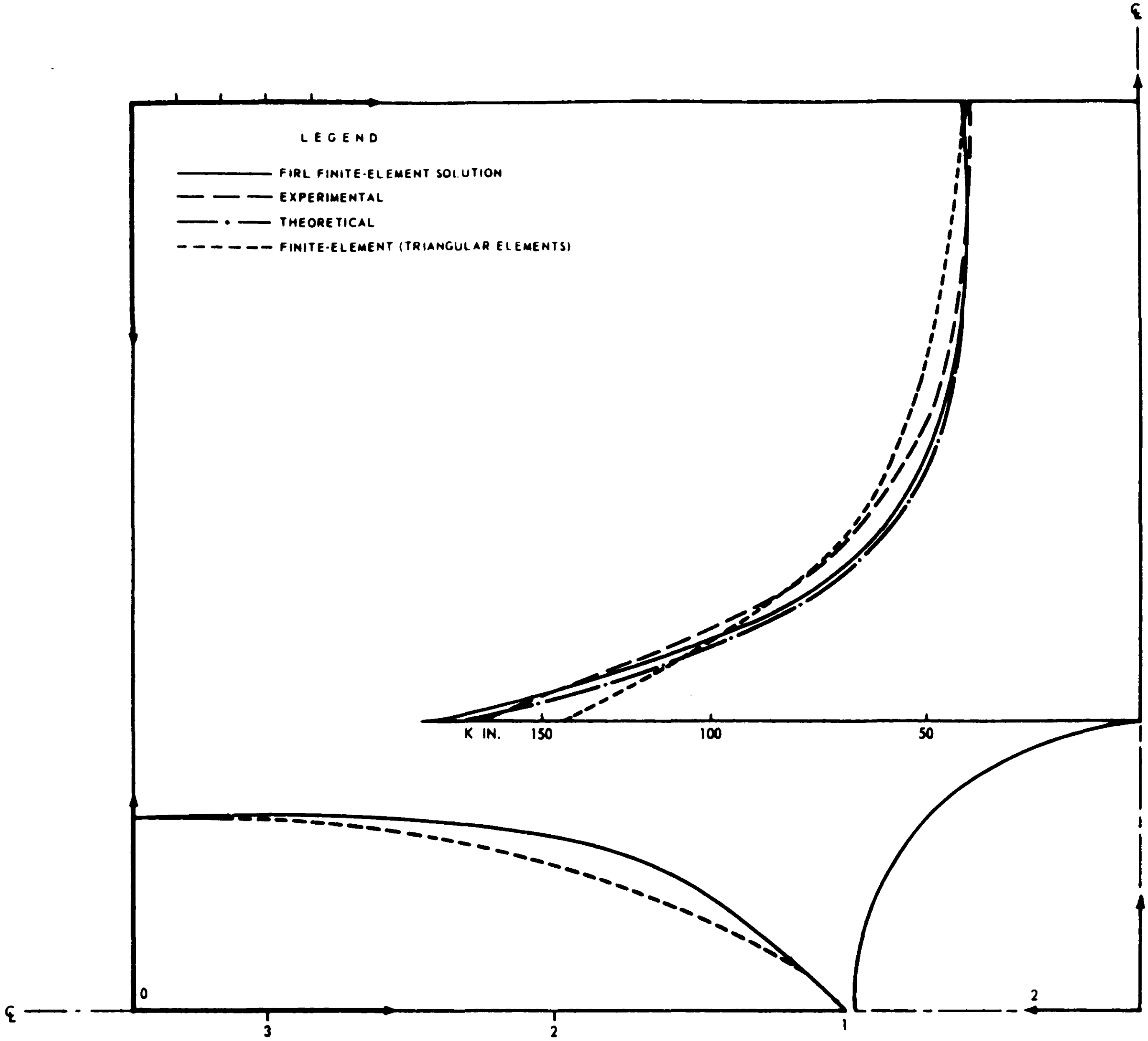

p. 5C.FIG-10

GPU Nuclear **Update -1**

TMI Unit-1 **7/82**

Hoop Stress - Resultant N_{θ} along Symmetry Axes (Test problem)

Fig. 5C-10

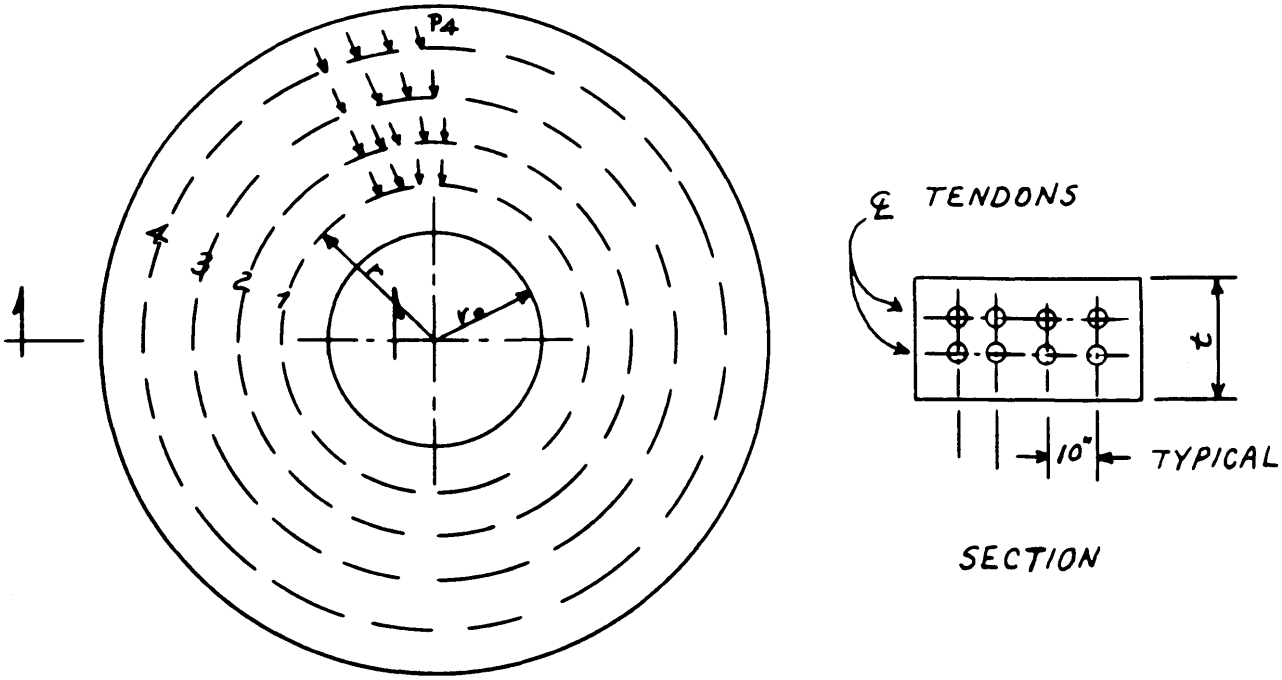

WHERE THE TERMS ARE IDENTIFIED AS FOLLOWS:

r_o = 11'-2" r = VARIABLE LEAST RADIUS OF DRAPED TENDONS

t = 84" P = RADIAL TENDON FORCE

p. 5C.FIG-11

GPU Nuclear | Update -1
TMI Unit-1 | 7/82

Effect of Tendon Curvature

Fig. 5C-11

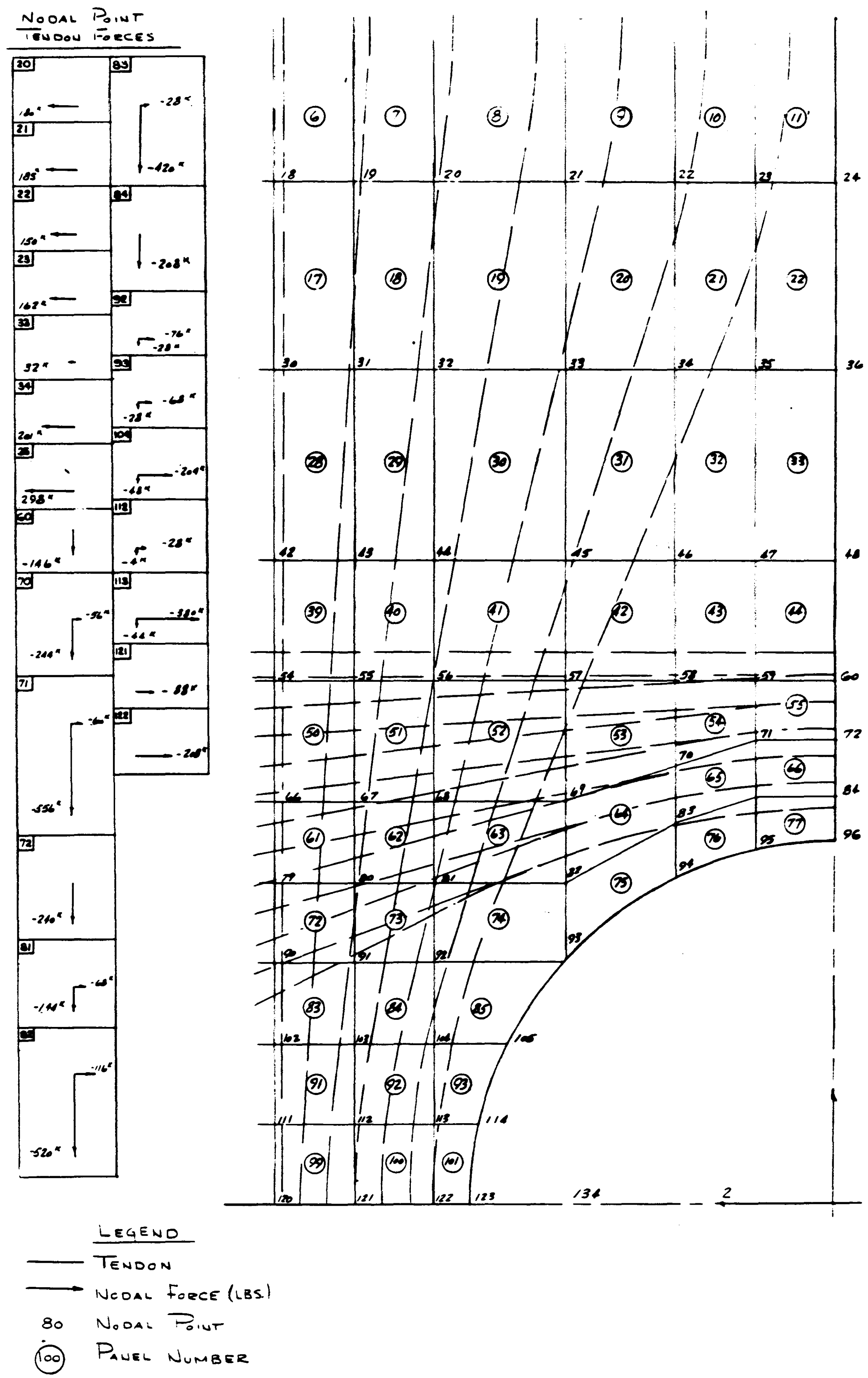

GPU Nuclear Update -1

TMI Unit-1 7/82

Nodal Forces Due to Curvature of Tendons in Neighborhood of Opening

Fig. 5C-12

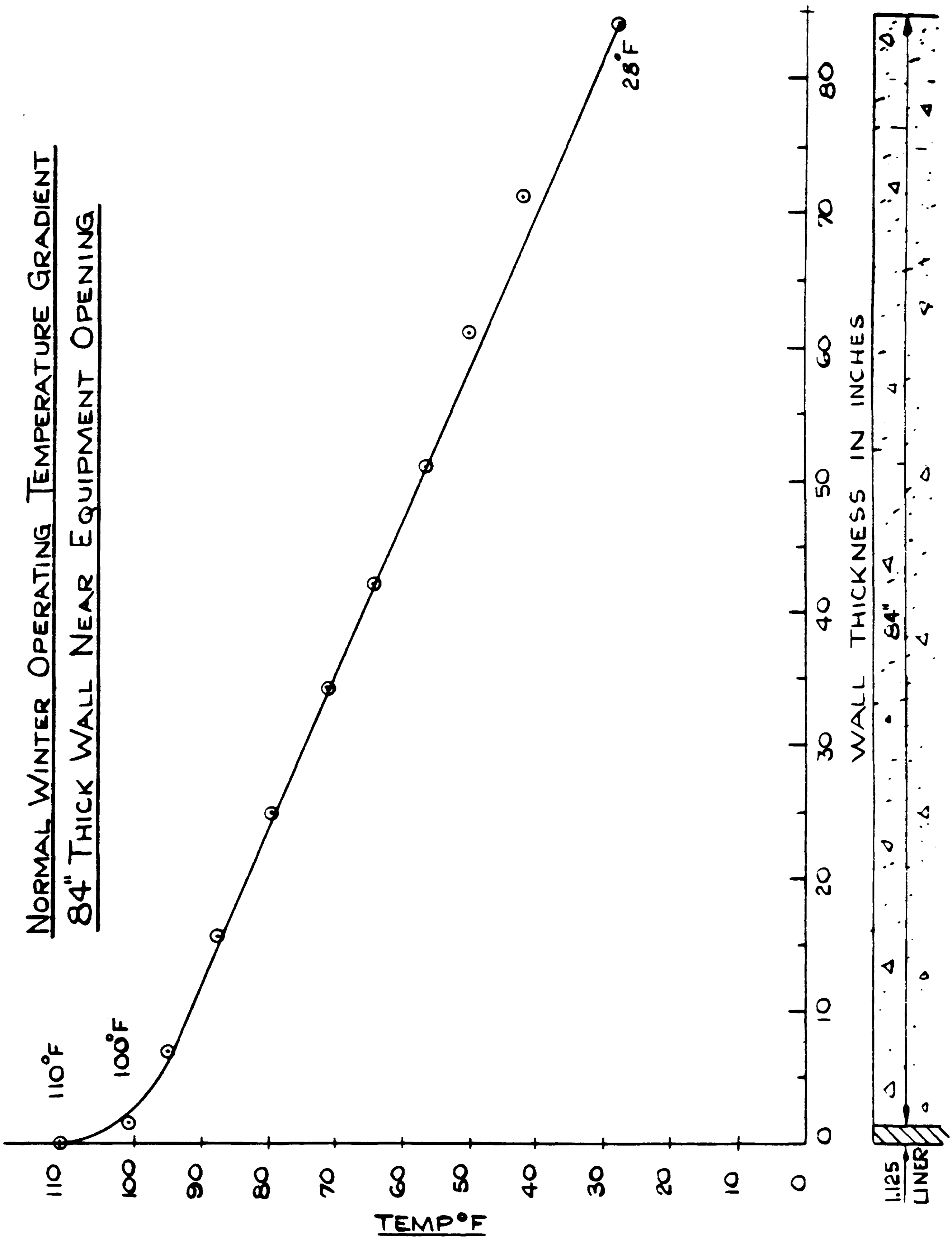

GPU Nuclear **Update -1**

TMI Unit-1 **7/82**

Normal Winter Operating Temperature Gradient - 84" Thick Wall Near Equipment Opening

Fig. 5C-13

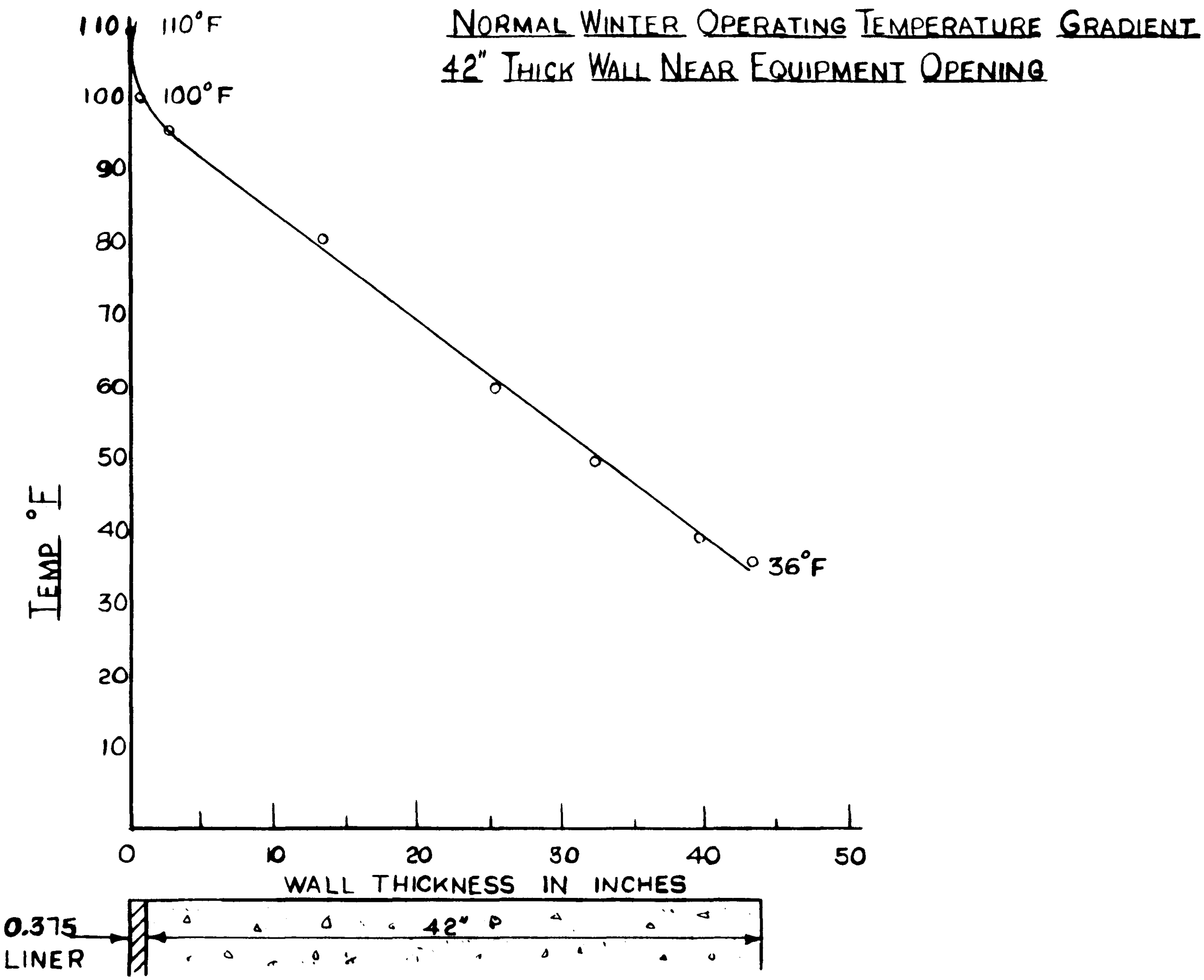

p. 5C.FIG-14

GPU Nuclear **Update -1**

TMI Unit-1 **7/82**

Normal Winter Operating Temperature Gradient - 42" Thick Wall Near Equipment Opening

Fig. 5C-14

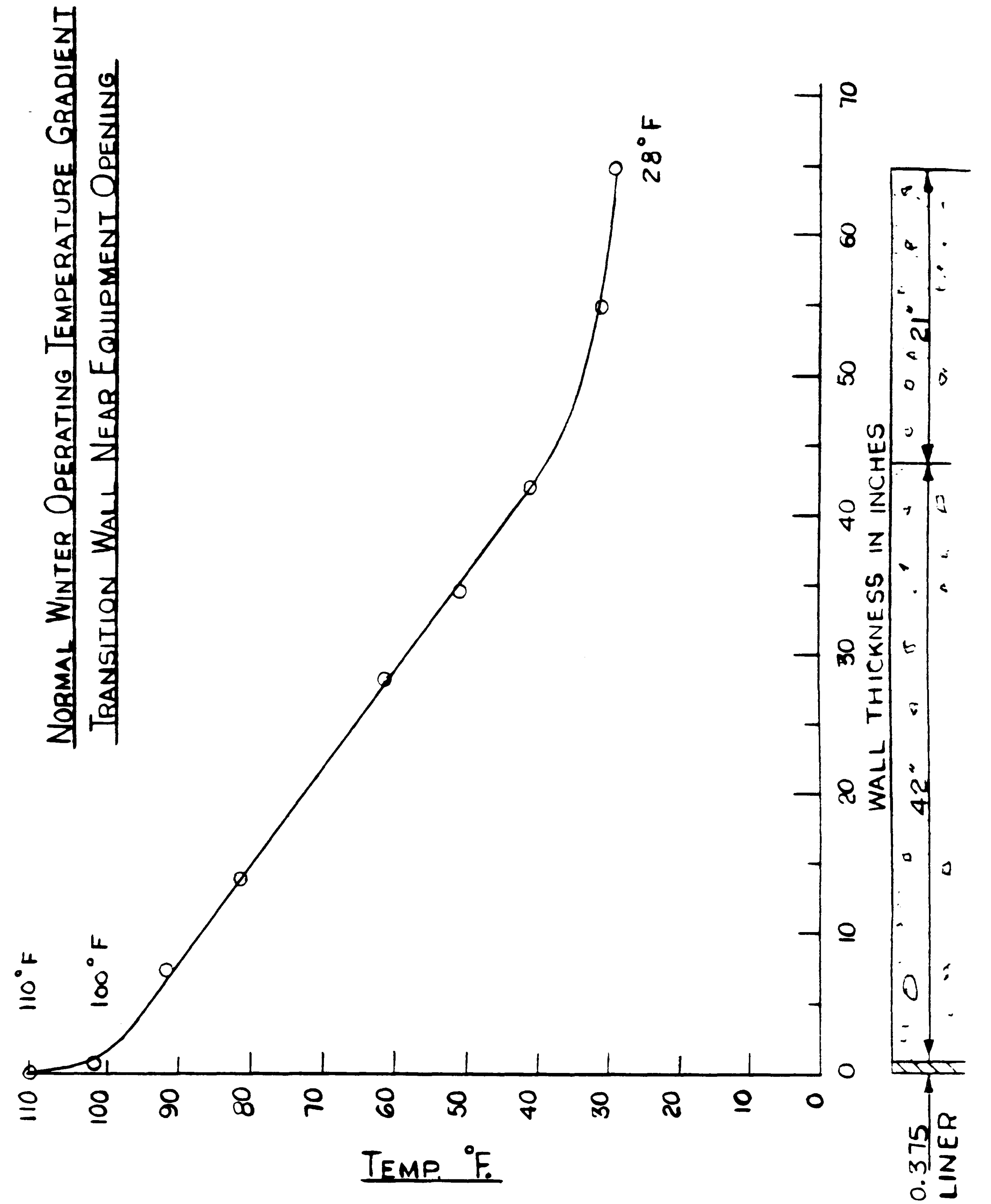

p. 5C.FIG-15

GPU Nuclear **Update -1**

TMI Unit-1 **7/82**

Normal Winter Operating Temperature Gradient - Transition Wall Near Equipment Opening

Fig. 5C-15

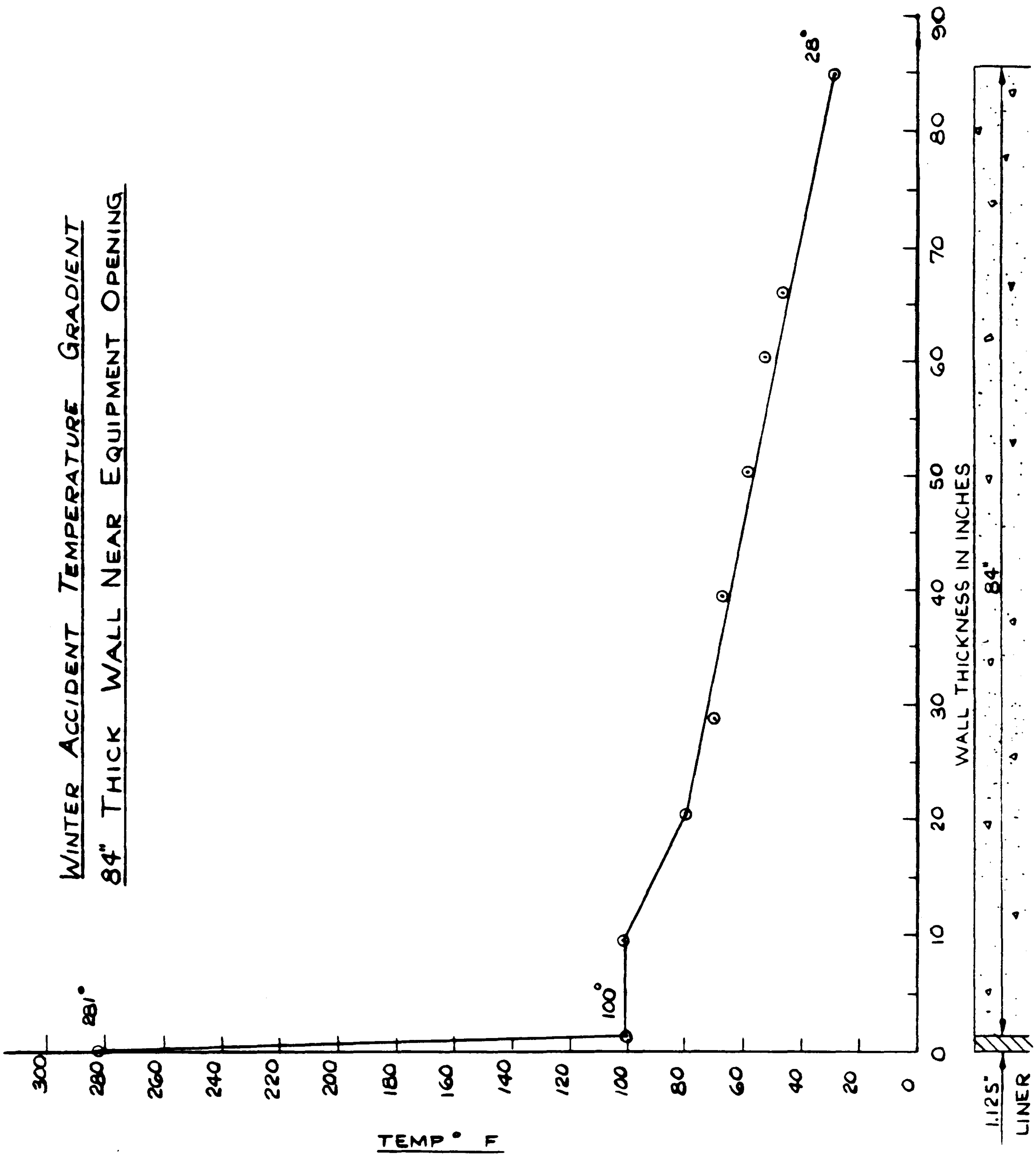

GPU Nuclear **Update -1**

TMI Unit-1 **7/82**

Winter Accident Temperature Gradient - 84" Thick Wall Near Equipment Opening

Fig. 5C-16

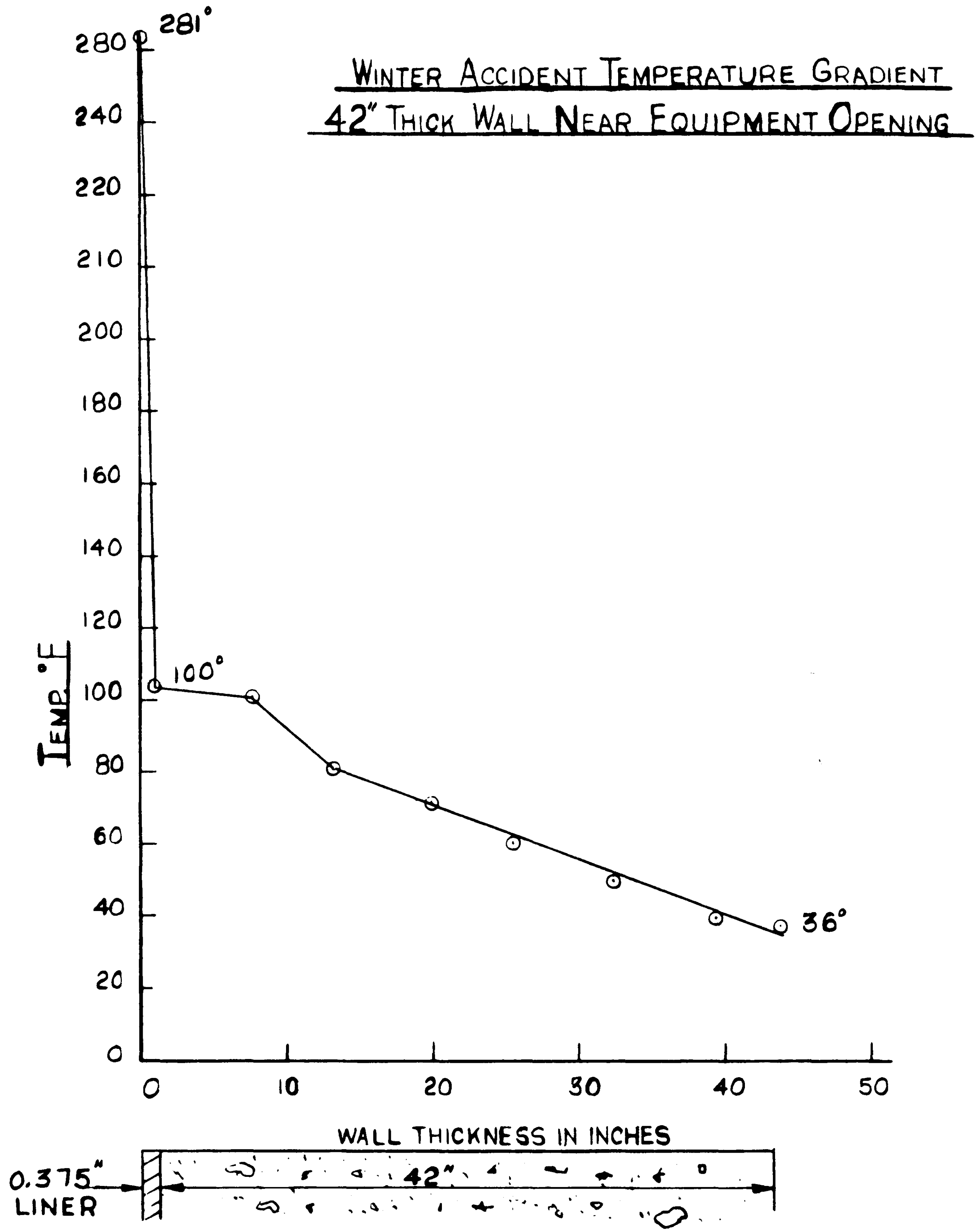

GPU Nuclear

Update -1

TMI Unit-1

7/82

Winter Accident Temperature Gradient - 42" Thick Wall Near Equipment Opening

Fig. 5C-17

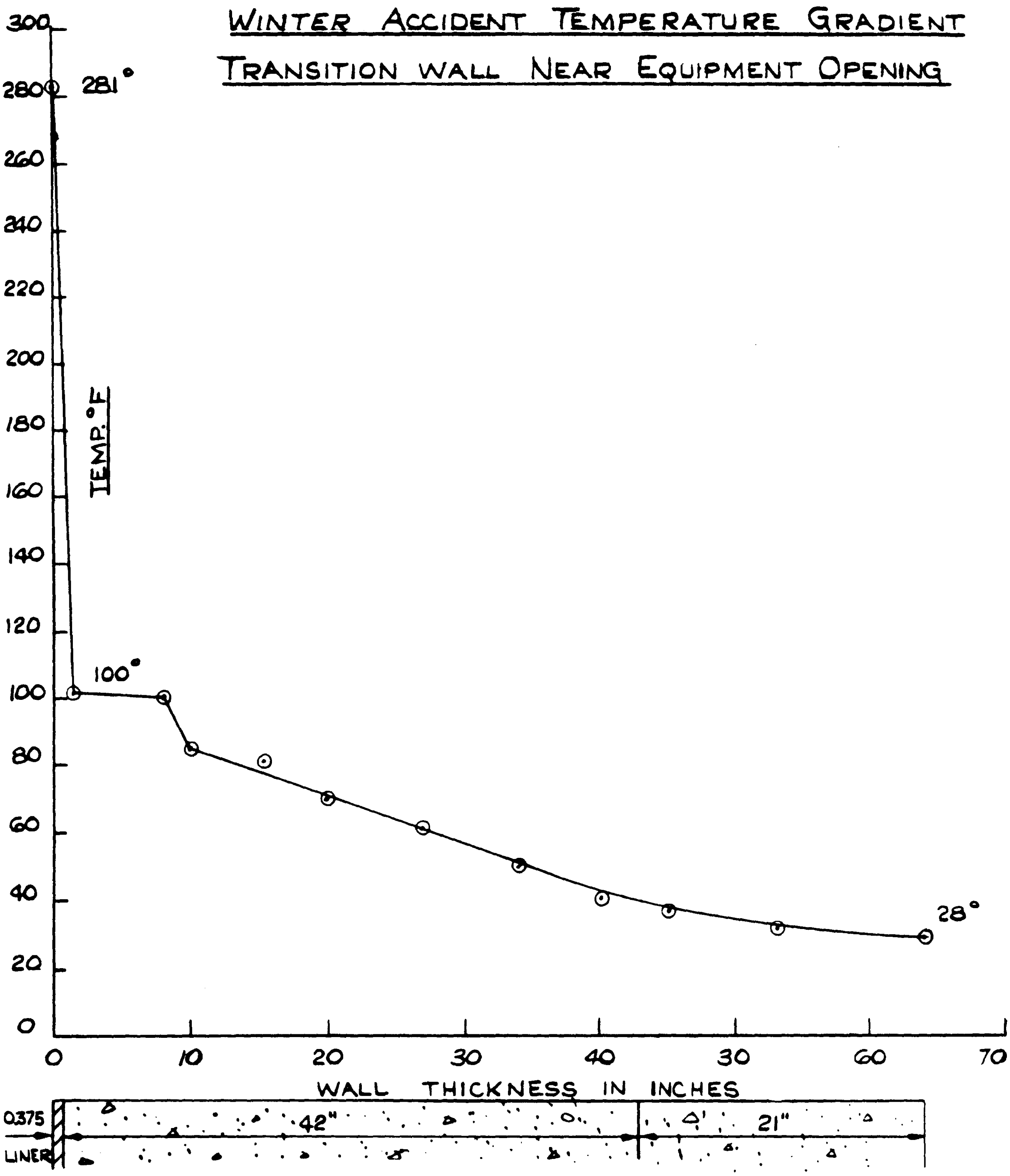

GPU Nuclear — **Update -1**

TMI Unit-1 — **7/82**

Winter Accident Temperature Gradient - Transition Wall Near Equipment Opening

Fig. 5C-18

INTERACTION DIAGRAM FOR AXIAL COMPRESSION/TENSION AND BENDING

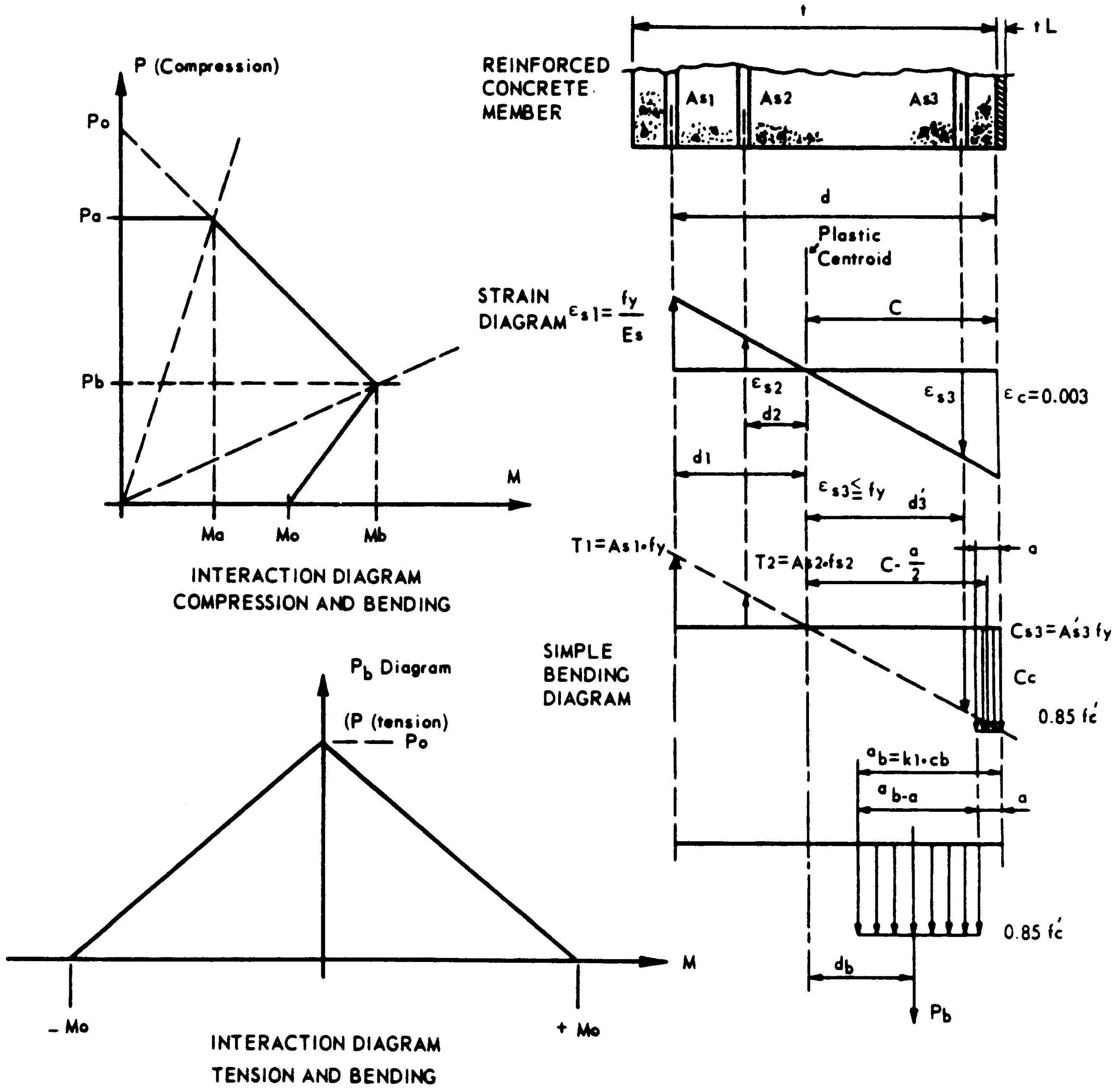

GPU Nuclear	**Update -1**
TMI Unit-1	**7/82**

Interaction Diagram for Axial Compression/Tension and Bending

Fig. 5C-19

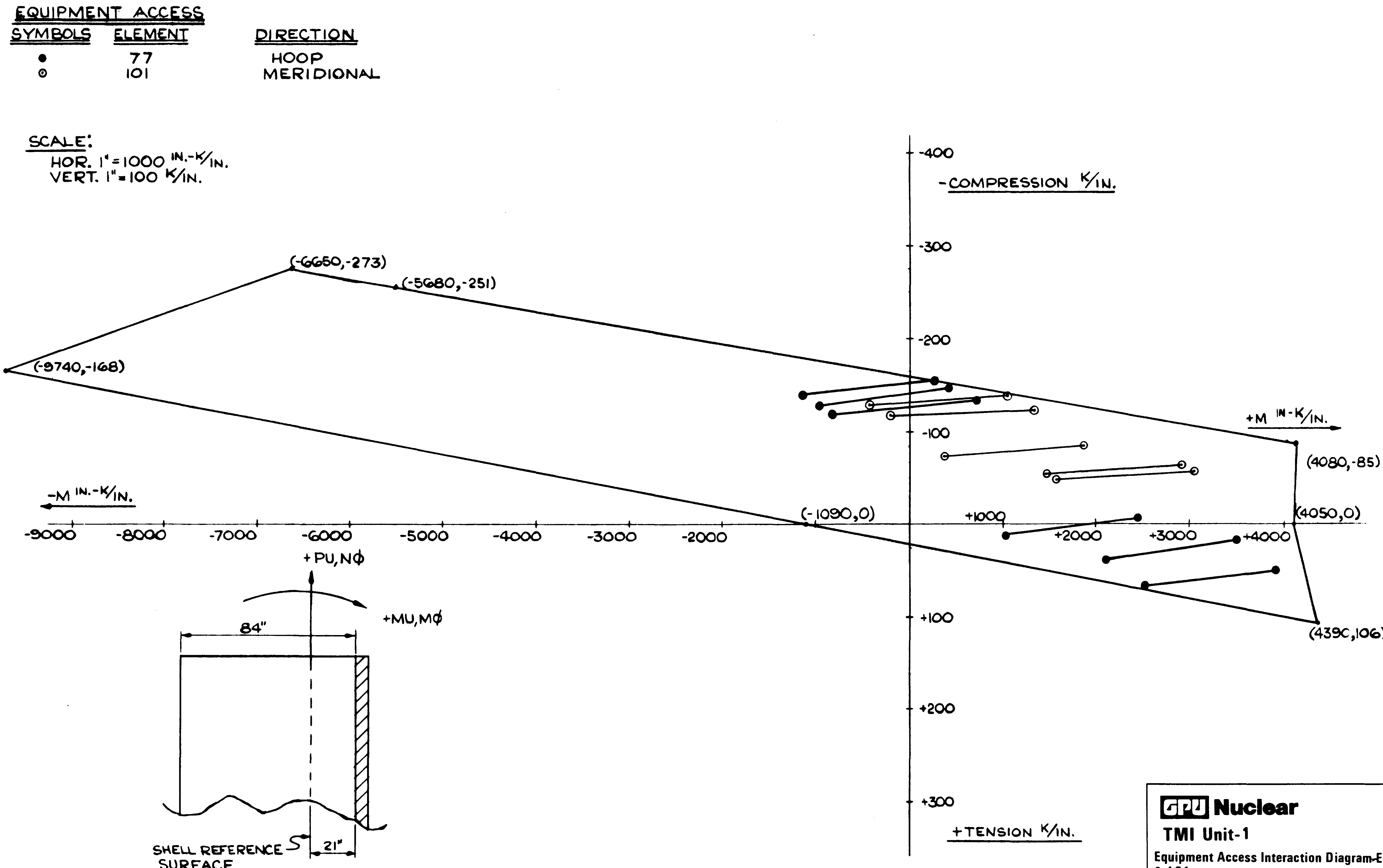

p. 5C.FIG-20

GPU Nuclear — Update -1

TMI Unit-1 — 7/82

Equipment Access Interaction Diagram-Elements 77 & 101

Fig. 5C-20

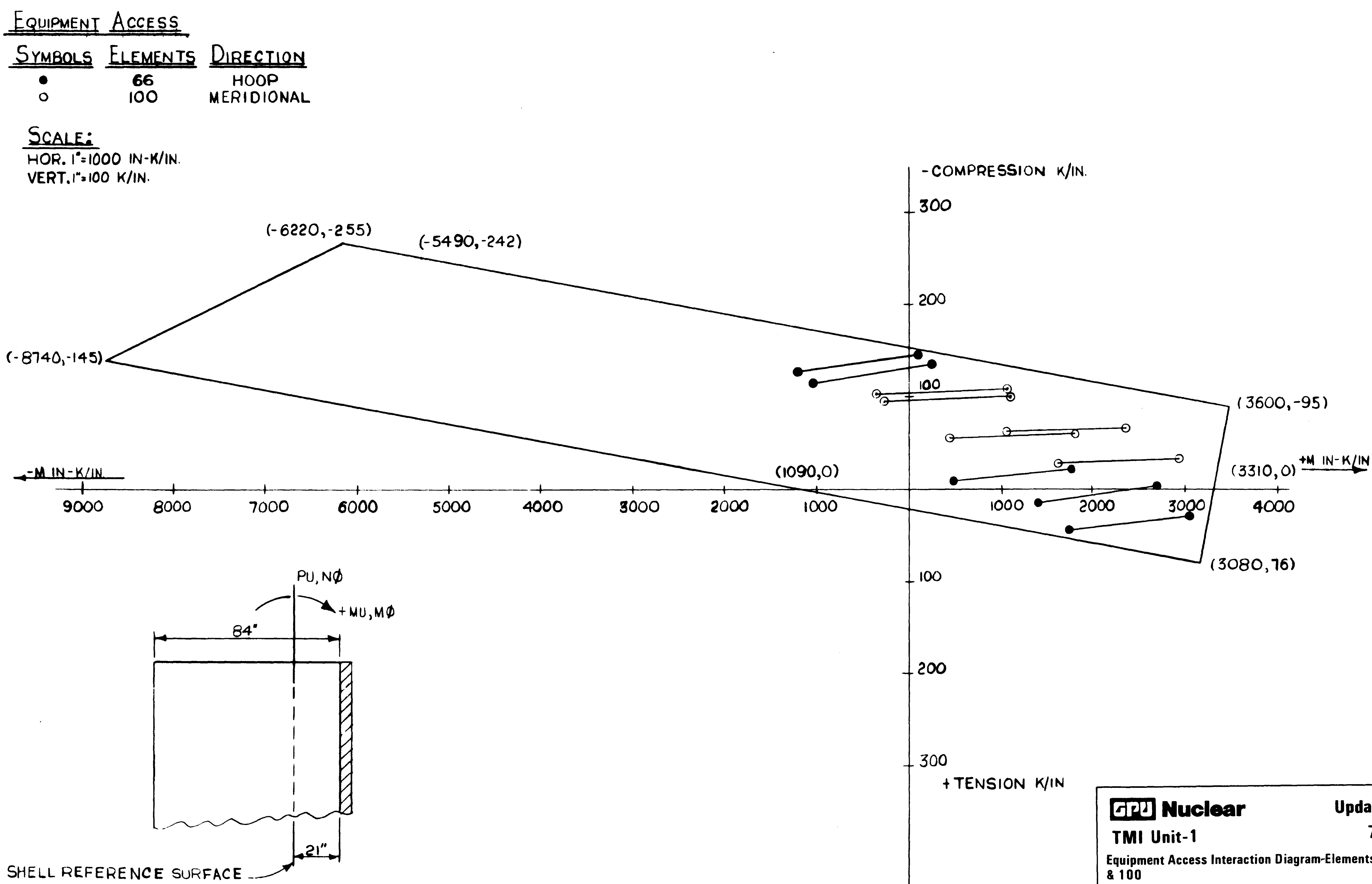

GPU Nuclear Update -1

TMI Unit-1 7/82

Equipment Access Interaction Diagram-Elements 66 & 100

Fig. 5C-21

EQUIPMENT ACCESS

SYMBOL	ELEMENT	DIRECTION
●	55	HOOP
⊙	99	MERIDIONAL

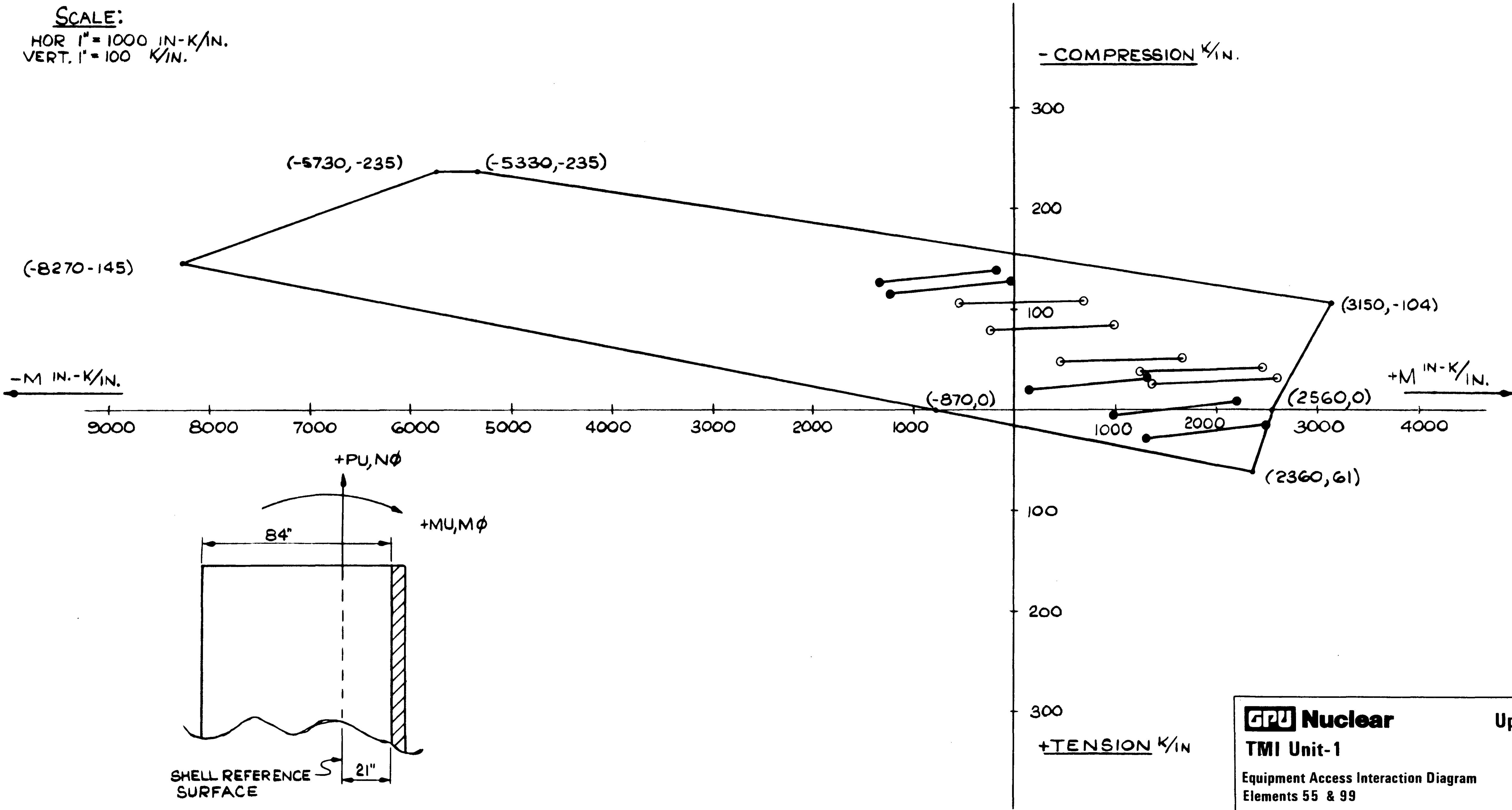

GPU Nuclear Update -1

TMI Unit-1 7/82

Equipment Access Interaction Diagram
Elements 55 & 99

Fig. 5C-22

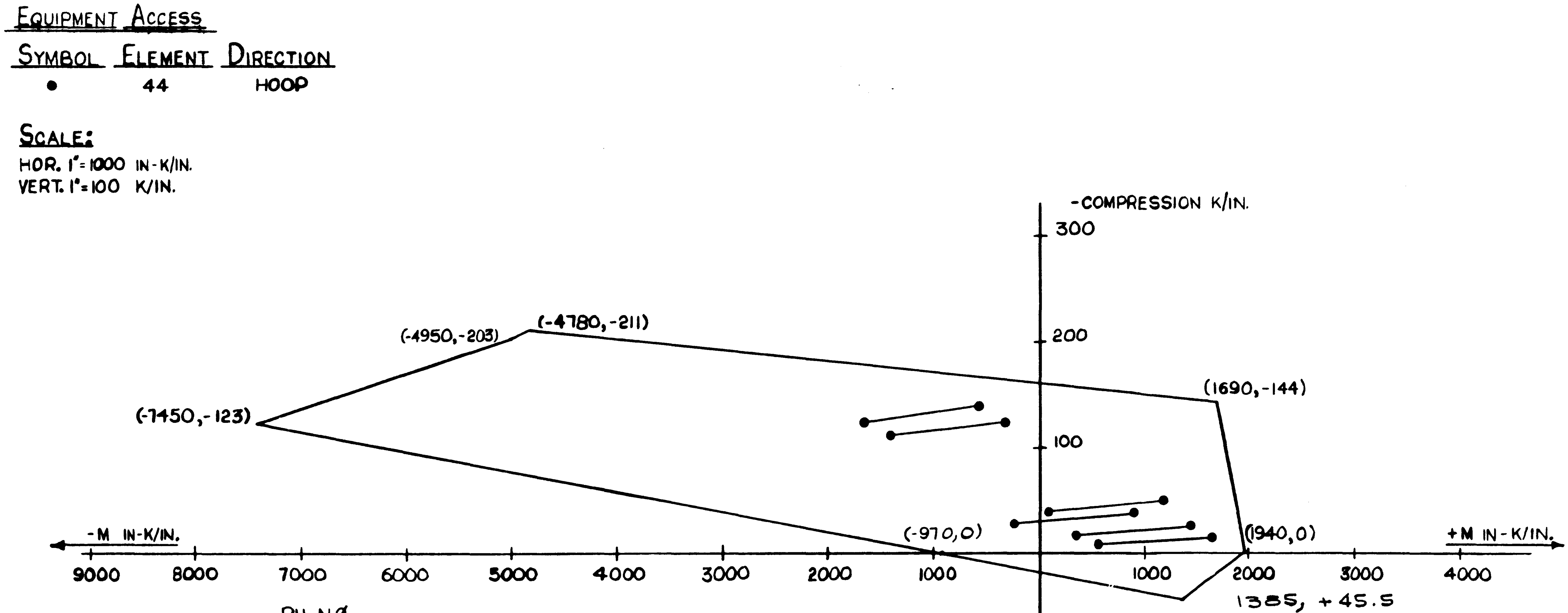

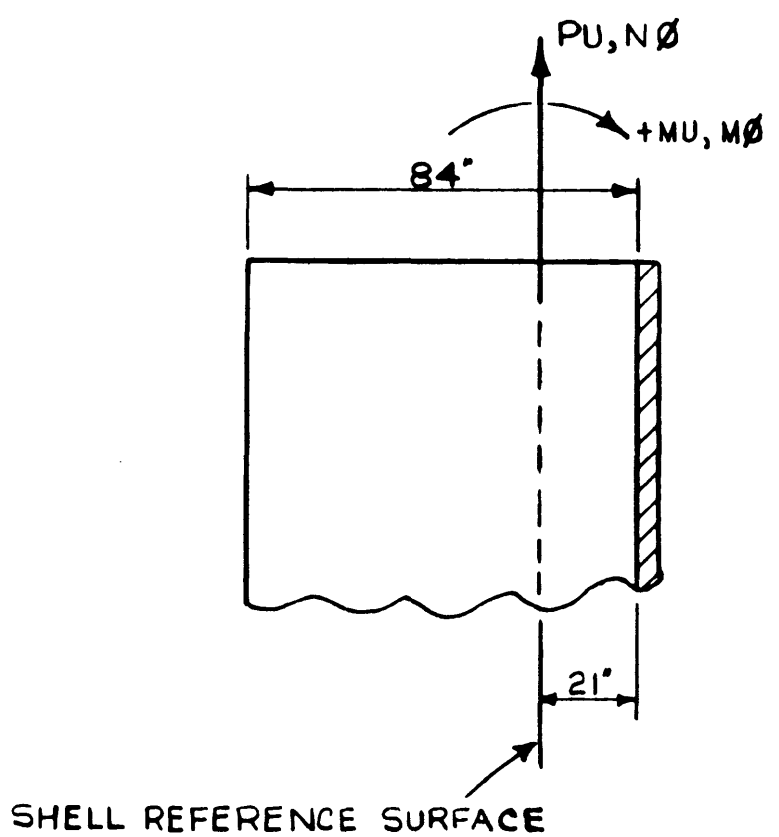

GPU Nuclear Update -1
TMI Unit-1 7/82

Equipment Access Interaction Diagram Element 44

Fig. 5C-23

EQUIPMENT ACCESS

SYMBOL	ELEMENT	DIRECTION
•	73	HOOP

SCALE:
HOR. 1" = 1000 IN. K/IN.
VERT. 1" = 100 K/IN.

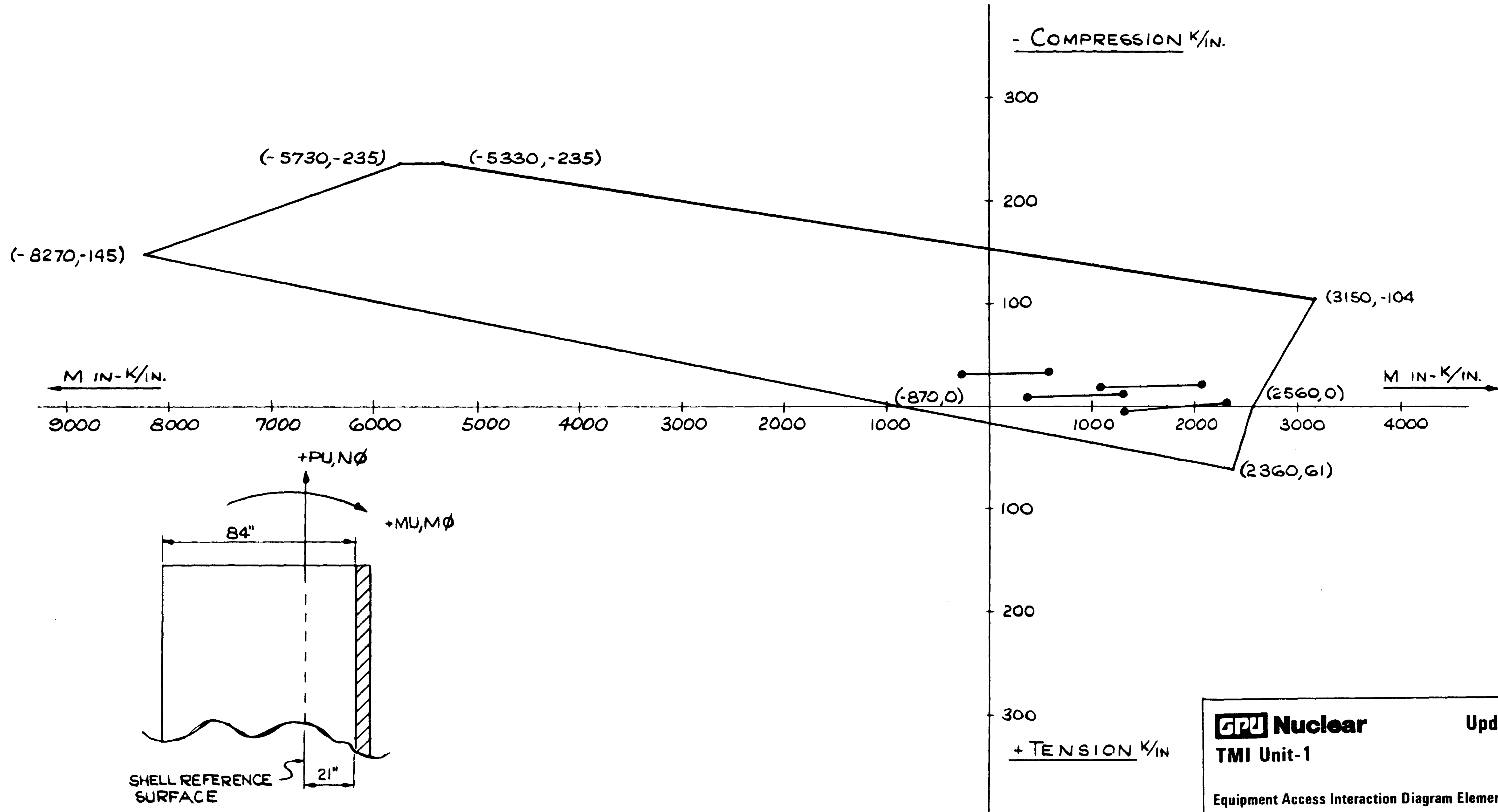

GPU Nuclear Update -1
TMI Unit-1 7/82

Equipment Access Interaction Diagram Element 73

Fig. 5C-24

EQUIPMENT ACCESS

SYMBOLS	ELEMENT	DIRECTION
●	74	HOOP

SCALE:
HOR. 1"=1000 IN-K/IN.
VERT. 1"=1000 K/IN.

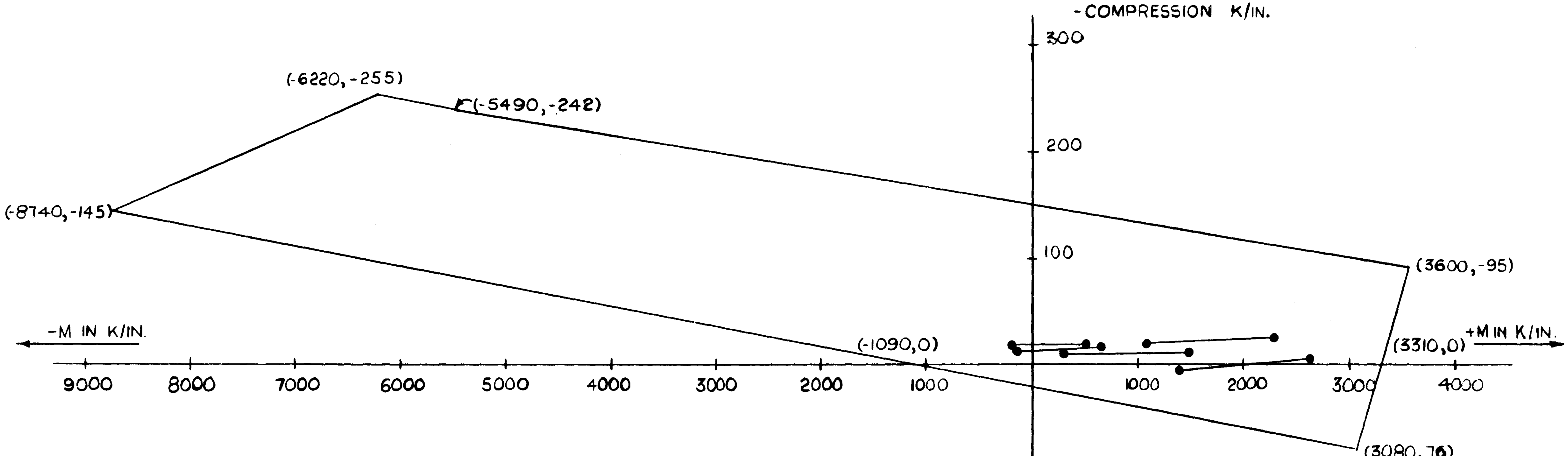

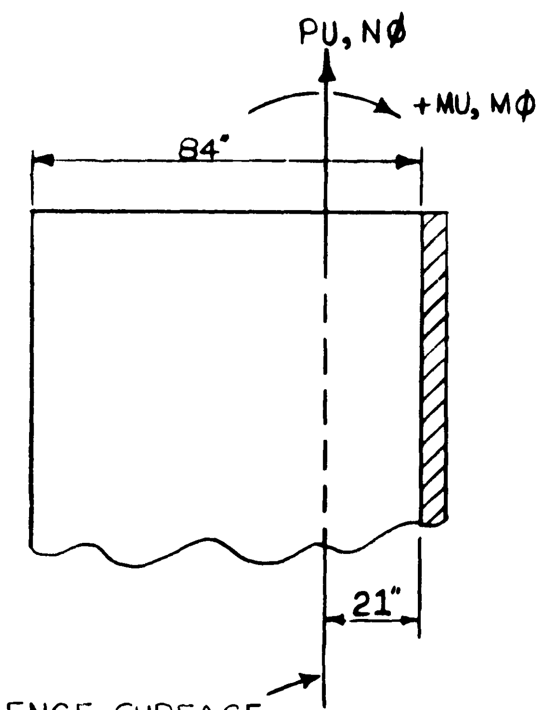

GPU Nuclear
TMI Unit-1
Update -1
7/82
Equipment Access Interaction Diagram Element 74
Fig. 5C-25

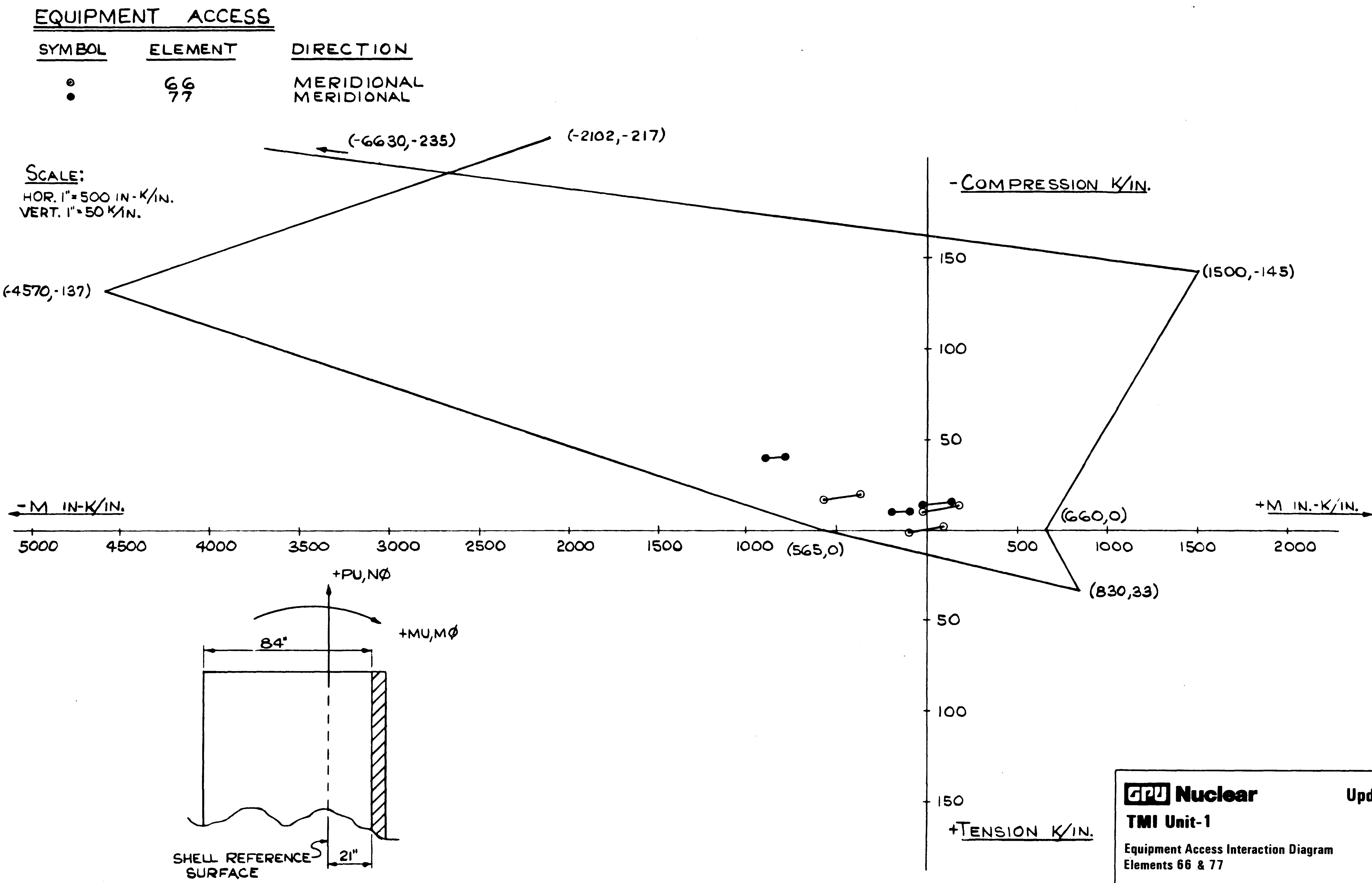

GPU Nuclear

TMI Unit-1

Update -1

7/82

Equipment Access Interaction Diagram
Elements 66 & 77

Fig. 5C-26

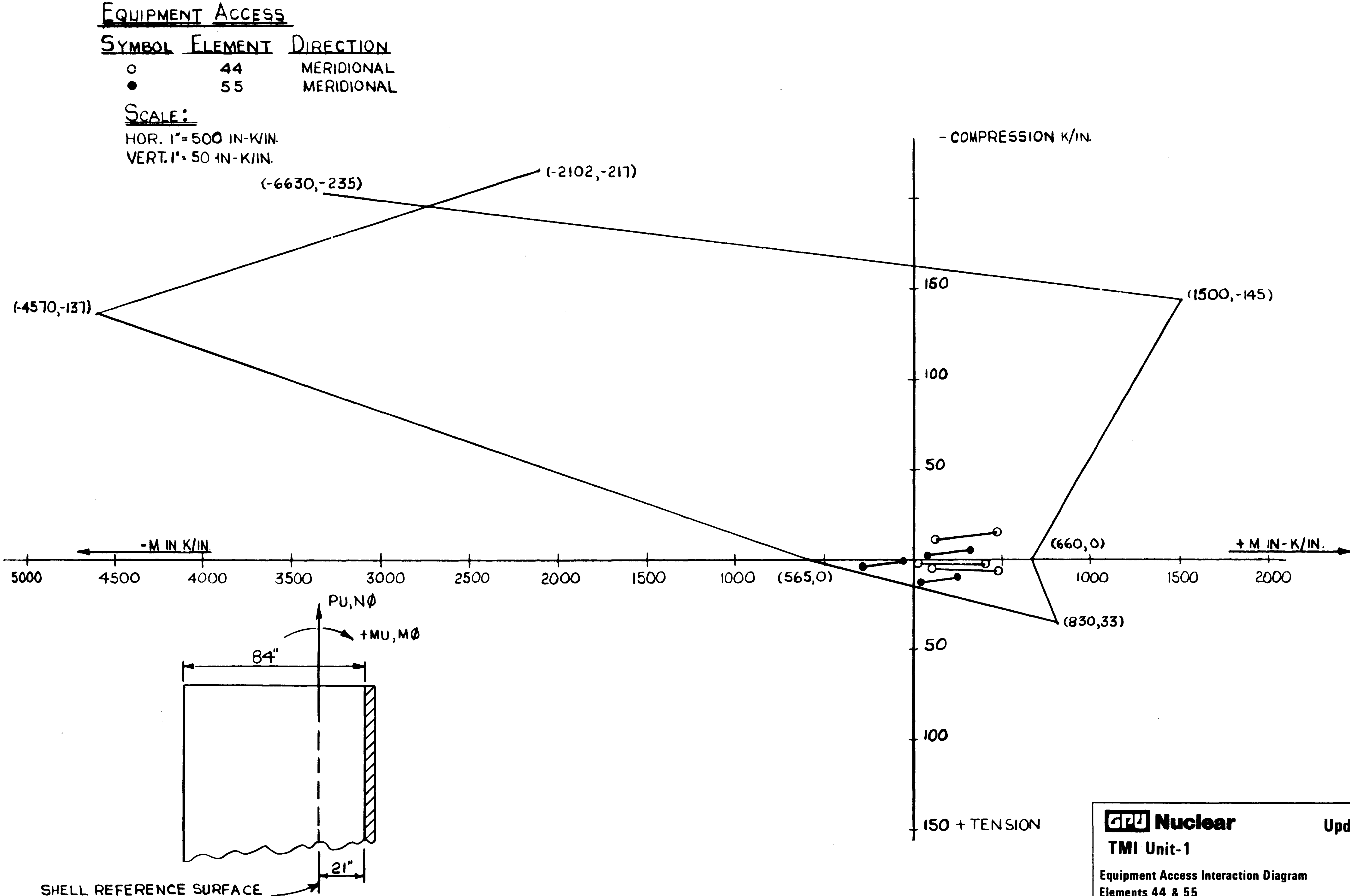

GPU Nuclear **Update - 1**

TMI Unit-1 **7/82**

Equipment Access Interaction Diagram
Elements 44 & 55

Fig. 5C-27

EQUIPMENT ACCESS

SYMBOL	ELEMENT	DIRECTION
⊙	99	HOOP
●	100	HOOP
△	101	HOOP

SCALE:
HOR. 1" = 1000 IN-K/IN
VERT. 1" = 100 K/IN

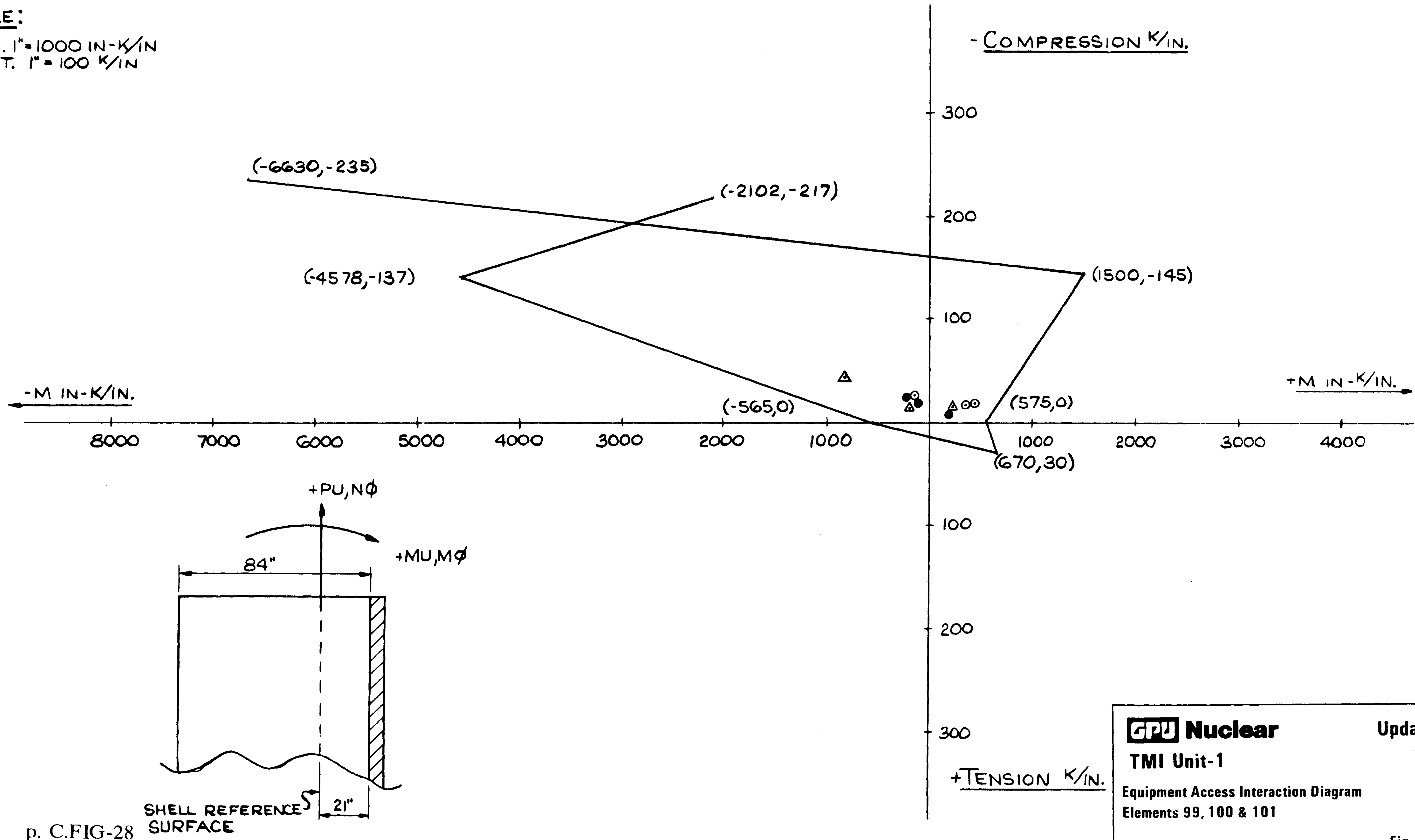

GPU Nuclear
TMI Unit-1
Update -1
7/82
Equipment Access Interaction Diagram
Elements 99, 100 & 101
Fig. 5C-28

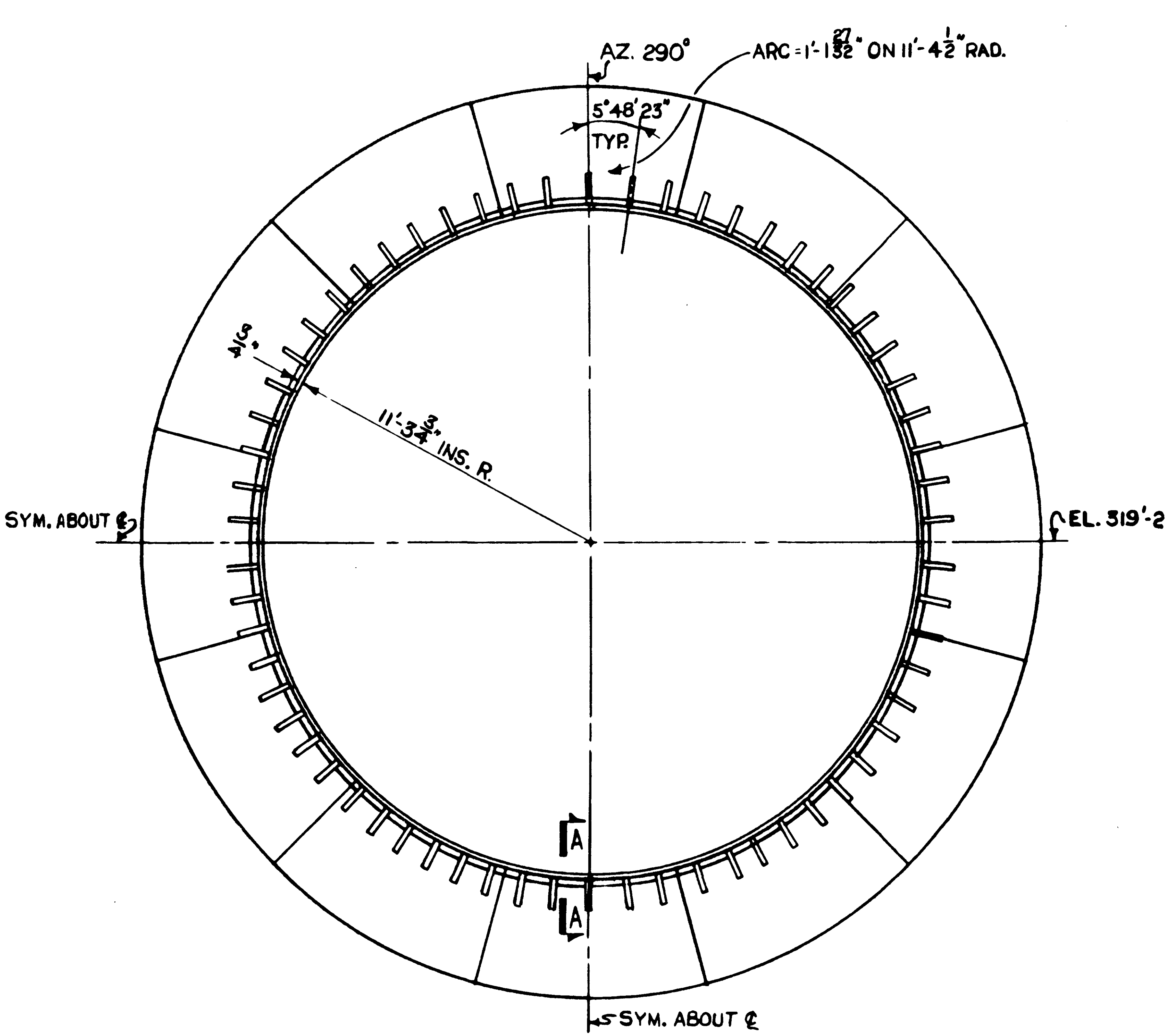

OUTSIDE ELEVATION VIEW

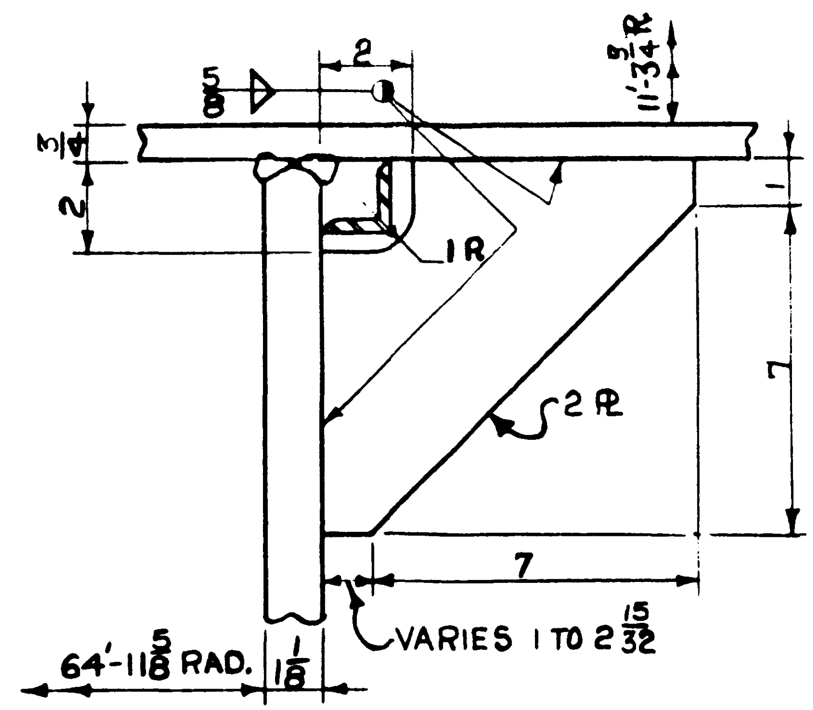

SECTION A-A

MATERIAL SPECIFICATION
℞-A516 GR. 70

GPU Nuclear
TMI Unit-1

Update -1
7/82

Sheer Transfer Plates

Fig. 5C-29